Aus der

Medizinischen Universitätsklinik und Poliklinik Tübingen

Abteilung Innere Medizin II

In vivo analysis of the role of BAALC overexpression in AML

Inaugural-Dissertation
zur Erlangung des Doktorgrades
der Medizin

der Medizinischen Fakultät
der Eberhard Karls Universität
zu Tübingen

vorgelegt von

Mardan, Jehan

2025

Dekan: Professor Dr. B. Pichler

1. Berichterstatter: Professorin Dr. J. Skokowa, Ph.D
2. Berichterstatter: Professor Dr. M. Ebinger

Tag der Disputation: 30.07.2025

für meine geliebten Eltern
Gülsan und Jamal Mardan

„Du glaubst dich aus dem Nichts und enthältst das Universum.“

- Avicenna (Ibn Sina)

Table of contents

I. Abbreviations

AML1-ETO ..... *Acute myeloid leukemia 1 - Eight-twenty-one*
ANC ..... *absolute neutrophil count*
BAALC ..... *brain and acute leukemia, cytoplasmatic*
CBF-AML ..... *core-binding factor AML*
CFSE ..... *Carboxyfluorescein succinimidyl ester*
CN ..... *Congenital neutropenia*
CN/AML ..... *congenital neutropenia/ acute myeloid leukemia*
CR ..... *complete remission*
DFS ..... *disease-free survival*
ERK ..... *extracellular signal-regulated*
FAB ..... *French-American-British*
FCS ..... *Fetal bovine serum*
FLT3 ..... *FMS-like tyrosine kinase 3*
FLT3-ITD ..... *FLT3 internal tandem duplication*
G-CSF ..... *granulocyte-colony stimulating factor*
GFP ..... *green fluorescent protein*
GSEA ..... *gene set enrichment analysis*
HD ..... *healthy donor*
HLTM ..... *human long-term culture medium*
HMA ..... *hypomethylating agents*
HPSC ..... *hematopoietic stem and progenitor cell*
HSCT ..... *hematopoietic stem cell transplantation*
iPSC ..... *Induced pluripotent stem cell*
KO ..... *knockout*
LSC ..... *leukemic stem cell*
MAP3K ..... *MAPK kinase kinase*
MAPK ..... Mitogen-activated protein kinase
MKP3 ..... *MAP kinase phosphatase 3*
MNC ..... *mononuclear cells*
NSG ..... *NOD scid gamma*

NTC ..... *No Template Control*

OS ..... *overall survival*

PAM ..... *Protospacer Adjacent Motif*

PBS ..... *Phosphate buffered saline*

PML-RARα ..... *Acute promyelocytic leukemia - Retinoic acid receptor, alpha*

RNP ..... *Ribonucleoprotein*, *ribonucleoprotein*

RT ..... *room temperature*

RUNX1 ..... *runt-related transcription factor 1*

*RUNX1-RUNX1*T1 ..... *RUNX1-RUNX1 Partner Transcritpitonal Co-Repressor 1*

SCN ..... *severe congenital neutropenia*

SCT ..... *stem cell transplantation*

sgRNA ..... *single guide RNA*

WHO ..... *World Health Organization*

WT ..... *wild type*

1. Introduction

1.1. Leukemia

Leukemia is a malignant disease of the hematopoietic system. In Germany, leukemia represented approximately 2,4% of newly diagnosed malignant diseases in women and 3,0% in men in 2020. Of the deaths due to malignant diseases, leukemia accounted for 3.4% to 3.8%.[1]

The disease is defined by an increase in the number of undifferentiated so-called leukemic blasts and a decrease in functional hematopoiesis. The unregulated proliferation of leukemic blasts leads to peripheral leukocytosis on the one hand and the repression of the hematopoietic islands in the bone marrow on the other. Bone marrow insufficiency usually leads to a variety of clinical manifestations. Patients suffer from a tendency to bleed due to thrombocytopenia, a higher vulnerability for infectious diseases due to neutropenia, as well as anemia due to erythrocytopenia. [2]

Although these characteristics link diverse types of leukemia, leukemia is a generic term for various diseases. They differ in etiology, epidemiology, therapy, and prognosis. Leukemia is categorized by the dynamics of the disease in acute and chronic and by the line of affected hematopoietic progenitor cells into myeloid and lymphoid. Acute leukemia typically shows a rapid onset and a progressive development, whereas chronic leukemia presents itself with a creeping onset and a slow progression. [2]

1.2. Acute myeloid leukemia

Acute myeloid leukemia (AML) accounts for approximately 24% of all adult leukemias and, thereby, is the second most common subtype of adult leukemia in Germany [1]. In children, it only represents 15-20% of newly diagnosed cases of acute leukemia [3].

The median age of diagnosis is 72 years. With 3-4 per 100.000 inhabitants per year newly diagnosed in Germany, AML is a relatively rare disease; nonetheless, AML has the highest mortality rate of all subtypes of leukemia, with a five-year survival rate of only 22-24% in adults. [1]

1.2.1. Classification of AML

A group of seven French, American, and British hematologists proposed six (later eight) objectively distinguishable subgroups of AML in 1976. The eight subtypes were differentiated based on morphological and cytochemical characteristics. [4-6](see table 1). Despite the developments in research regarding AML classification, the French-American-British (FAB) classification is still used in research and applied medicine.

TABLE 1: FAB CLASSIFICATION OF AML

M0	minimally differentiated acute myeloid leukemia
M1	myeloblastic leukemia without maturation
M2	myeloblastic leukemia with maturation
M3	promyelocytic leukemia
M4	myelomonocytic leukemia
M5	monocytic leukemia
M6	erythroleukemia
M7	acute leukemia of megakaryocyte lineage

A new classification of AML was presented by the World Health Organization (WHO) in the year 2001 and has been updated four times since then. The 5th WHO classification emphasizes genetic information but also includes morphology, immunophenotype, and clinical presentation in its approach to distinguishing between subgroups of AML. The two main categories and the containing undercategories are listed in table 2. [7-9]

TABLE 2: 5th WHO CLASSIFICATION OF AML 2022 [8]

AML with defining genetic abnormalities

- Acute promyelocytic leukemia with PML::RARA fusion
- AML with *RUNX1::RUNX1T1* fusion
- AML with *CBFB::MYH11* fusion
- AML with *DEK::NUP214* fusion
- AML with *RBM15::MRTFA* fusion
- AML with *BCR::ABL1* fusion
- AML with *KMT2A* rearrangement
- AML with *MECOM* rearrangement
- AML with *NUP98* rearrangement
- AML with *NPM1* mutation
- AML with *CEBPA* mutation
- AML, myelodysplasia-related (AML-MR)

  Defining cytogenetic abnormalities in AML-MR:
  - Complex karyotype (≥ 3 abnormalities)
  - 5q deletion or loss of 5q due to unbalanced translocation
  - Monosomy 7, 7q deletion, or loss of 7q due to unbalanced translocation
  - 11q deletion
  - 12p deletion or loss of 12p due to unbalanced translocation
  - Monosomy 13 or 13q deletion
  - 17p deletion or loss of 17p due to unbalanced translocation
  - Isochromosome 17q
  - idic(X)(q13)

  Defining somatic mutations in AML-MR:
  - *ASXL1*
  - *BCOR*
  - *EZH2*
  - *SF3B1*
  - *SRSF2*

- *STAG2*
- *U2AF1*
- *ZRSR2*

- AML with other defined genetic alterations

AML, defined by differentiation

- AML with minimal differentiation
- AML without maturation
- AML with maturation
- Acute basophilic leukemia
- Acute myelomonocytic leukemia
- Acute monocytic leukemia
- Acute erythroid leukemia
- Acute megakaryoblastic leukemia

1.2.2. Pathogenesis of AML

Numerous events can lead to the irregular proliferation and differentiation of a clonal population of the myeloid lineage from a hematopoietic stem and/or progenitor cell (HSPC), causing the clinical appearance of AML. [10]

Almost thirty years ago, the researchers Bonnet and Dick formulated the leukemia stem cell model. They described a subpopulation of cells with $CD34^{++}CD38^{-}$ surface markers, which had not only the ability to induce AML *in vivo* but were also capable of limitless self-renewal and had the characteristics of stem cells regarding proliferation and differentiation. [11]

Like hematopoietic stem cells, leukemic stem cells (LSC) are considered to reside in the bone marrow rather than the blood circulation. The microenvironment of LSCs in the bone marrow is often referred to as the niche in research literature. Strong evidence suggests that LSCs are protected from the cytotoxic effects of chemotherapy in the bone marrow niche and, therefore, are able to initiate relapse. [12]

According to current understanding, LSCs derive from hematopoietic stem cells or progenitor cells by acquiring one or more transforming mutations.[13]

In the often proposed ‘two-hit’ model of leukemogenesis, two different mutations must occur to initiate leukemia. A cooperativity of class I mutations, which trigger an increase in proliferation, and class II mutations, which impede differentiation. [14]

Chromosomal alterations and molecular genetic mutations are the leading causes of the pathogenesis of AML. Chromosomal translocations like t(8;21), inv(16), or t(16;16), among other events, induce the core-binding factor AML (*CBF-AML*). Another example is translocation t(15;17), found in acute promyelocytic leukemia (APL). Translocations like these often lead to fusion genes and resulting fusion proteins. T(8;21) causes the appearance of the fusion oncogene *Runt-related transcription factor 1 - RUNX1 Partner Transcriptional Co-Repressor 1* (*RUNX1-RUNX1*T1 previously called *Acute myeloid leukemia 1 - Eight-twenty-one* (*AML1-ETO*). The translocation t(15;17) triggers the synthesis of the fusion gene *Acute promyelocytic leukemia - Retinoic acid receptor, alpha* (*PML-RARα*). *AML1-ETO* and *PML-RARα* hinder the transcription of specific target genes, whereby proteins that are essential for the differentiation of myeloid cells lack. Mutations leading to fusion genes like *AML1-ETO* and *PML-RARα* can be categorized as class II mutations. The most common class II mutation is the mutation of the *NPM1* gene. Important examples of class I mutations are mutations of receptor tyrosine kinases *FMS-like tyrosine kinase 3* (*FLT3*) and *c-KIT*. Mutation of *FLT3* is the most common class I mutation in AML patients. [10]

Additionally to these two classes of mutations, a third kind of genetic alteration has been established as an actor in the development of AML: mutations in epigenetic regulator genes. These mutations have downstream effects on differentiation as well as proliferation. This category includes *DNMT3A*, *TET2*, *IDH-1*, and *IDH-2,* which concern DNA-methylation. [15]

AML has been found to have a small number of genetic mutations compared to other malignant diseases, with an average of 13 mutations per case. 97% of AML have at least one driver mutation. [16]

Although the pathogenesis of AML is much better understood today than two decades ago, there is still a lot of uncertainty in this field, such as the link between the identified mutations. [10]

While most AML develops as a de novo malignancy, a third of AML are either therapy-related AML, which occurs after genotoxic chemo- or radiotherapy, or associated with antecedent hematologic disease (AHD), such as myelodysplastic syndrome (MDS) or myelodysplastic/myeloproliferative neoplasm. [17]

Severe congenital neutropenia is such a hematologic disorder that can lead to secondary AML.

1.2.3. MDS/AML associated with severe congenital neutropenia

Congenital neutropenia (CN) is a rare disease of the hematopoietic system defined by impaired myelopoiesis leading to chronic neutropenia recurring from birth. Neutrophile granulocytes are essential immune cells. The disease can be categorized by absolute neutrophil count (ANC) in peripheral blood into mild (ANC between 1,0 and $1{,}8\times10^9$/L), intermediate (ANC between 0,5 and $1{,}0\times10^9$/L), and severe congenital neutropenia (ANC under $0{,}5\times10^9$/L). [18]

Patients with severe congenital neutropenia (SCN) typically present with symptoms associated with immunodeficiency, like infectious dermatitis, pneumonia, gingivitis, or even life-endangering bacterial sepsis. Around 50% of the patients show an autosomal dominant mutation in the gene that encodes for the neutrophile elastase *ELANE*. 11% of CN is caused by autosomal recessive mutations in the *HAX1* gene (in Europe). *HAX1* encodes for the HCLS1-associated protein X-1 (HAX-1), which is, among other things, critical in the activation of the granulocyte-colony stimulating factor (G-CSF) signaling pathway. Standard first-line therapy for congenital neutropenia is the injections of G-CSF. [18-20]

Patients with severe congenital neutropenia have a high risk of developing leukemia. The cumulative incidence of leukemia in SCN patients is estimated to be 22% after ten years [19, 21]. The term CN/AML is used for AML, which occurs in patients with previous (mostly severe) congenital neutropenia.

By analyzing mutations in CN/AML using next-generation deep-sequencing, Skokowa et al. found that two-thirds of 31 CN/AML patients acquired *RUNX1*

mutations. In contrast, in de novo AML, *RUNX1* mutations were rare. *RUNX1* encodes the transcription factor RUNX1, which is essential in myeloid hematopoiesis. *RUNX1* mutations were found to be late incidents in leukemic transformation of CN into CN/AML. Of the CN patients with *RUNX1* mutations, approximately 80% showed mutations in the gene that encodes for the colony stimulating factor 3 receptor in granulocytes: *CSF3R.* The high number of CN/AML patients with *CSF3R* and *RUNX1* mutations suggests these mutations play a cooperative role in leukemogenesis.[22, 23]

1.2.4. Prognosis of AML

AML with prior hematologic disease and therapy-related AML have a worse prognosis than de novo AML.[17]

Prognostic factors in AML are essential for the assessment of suitable therapeutic approaches for each patient. Patient groups older than 60 years and/or reduced general condition usually achieve lower rates of complete remission (CR) and overall survival (OS). Based on the cytogenetic and molecular profile, AML can be categorized into three prognostic risk groups: favorable, intermediate, and adverse. Patients with CBF-AML hold a favorable prognosis, whereas patients with normal cytogenetics obtain an intermediate prognosis. Patients with karyotypes like monosomy-5 or -7 or complex karyotype have an adverse prognosis. [10, 24]

Most AML patients are cytogenetically normal (40 to 50%). The absence of chromosomal abnormalities complicates the risk stratification in these patients. Molecular markers have been discovered as a valuable option as prognostic factors in these cytogenetically normal patients, such as *FLT3* internal tandem duplication (*FLT3-ITD*), *NPM1* mutation, biallelic *CEBPA* mutation, partial tandem duplications within the *MLL* gene, *RUNX1* mutation, and *ASXL1* mutation. [25, 26]

The following table shows the risk stratification of AML by genetics of the European LeukemiaNet (ELN) from 2022 [27].

TABLE 3: ELN RISK STRATIFICATION BY GENETICS AT INITIAL DIAGNOSIS (2022)

Risk category	Genetic abnormality
Favorable	– t(8;21) (q22;q22.1); *RUNX1-RUNX1T1* – inv(16)(p13.1q22) or t(16;16)(p13.1;q22)/*CBFB-MYH11* – Mutated *NPM1* without *FLT3-ITD* – bZIP in frame mutated *CEBPA*
Intermediate	– Mutated *NPM1* and *FLT3-ITD* – Wild type *NPM1* without *FLT3-ITD* or with *FLT3-ITD*low (without adverse-risk genetic lesions) – t(9;11)(p21.3;q23.3); *MLLT3-KMT2A* – Cytogenetic abnormalities not classified as favorable or adverse
Adverse	– t(6;9)(p23;q34.1); *DEK-NUP214* – t (v;11q23.3); *KMT2A* rearranged – t (9;22) (q34.1;q11.2); *BCR-ABL1* – inv(3)(q21.3q26.2) or t(3;3)(q21.3;q26.2); *GATA2,MECOM(EVI1)* – t(3q26.2;v)/MECOM(EVI1)-rearranged – −5 or del(5q); −7; −17/abn(17p) – Complex karyotype, monosomal karyotype – Mutated *ASXL1, BCOR, EZH2, RUNX1, SF3BW, SRSF2, STAG2, U2AF1*, or *ZRSR2* – Mutated *TP53*

1.2.5. Treatment of AML

Treatment choice is based on the patient's respective pathophysiology, prognosis, and condition. In general, the therapy of AML consists of two phases of chemotherapy: induction therapy and consolidation.

The standard procedure of first-line induction therapy for AML is the ‘7+3’-regimen, which stipulates seven days of cytarabine (Ara-C) infusion and three days of anthracycline, such as daunorubicin or idarubicin. With this intensive induction therapy, CR is accomplished in 60-80% of patients below and 40-60% of patients above the age of 60. [26]

Consolidation regimens usually consist of single-agent cytarabine at high doses (up to four cycles) or multiagent chemotherapy. The consolidation chemotherapy is commonly followed by autologous or allogeneic hematopoietic stem cell transplantation (HSCT). [26]

Hypomethylating agents (HMAs), such as azacytidine, were found to be beneficial regarding OS in elderly AML patients or patients with an adverse cytogenetic-risk profile.[28]

Targeted therapies are a novel approach in the field of alternative systemic therapy that targets cancer cells with specific surface proteins or genetic mutations. Examples are the tyrosine kinase inhibitors Midostaurin or Sorafenib, which are used for AML patients with *FLT3* mutations; Gemtuzumab ozogamicin in combination with chemotherapy for cells with CD33 surface proteins; or inhibitors of the metabolic enzymes *IDH1* and *IDH2*, which are often mutated in AML patients. [10, 26]

1.3. *BAALC*

Brain and acute leukemia, cytoplasmatic (*BAALC*) is a human gene located on the long arm of chromosome 8. The gene is 90kb long, contains eight exons, and codes for the brain and acute leukemia, cytoplasmatic protein. *BAALC* is highly conserved in mammals and expressed in neuroectoderm-derived tissues as well as in CD34-positive progenitor cells from bone marrow. [29]

1.3.1. Role of *BAALC* in leukemogenesis

The distinct overexpression of *BAALC* in acute leukemia has led to further scientific investigations by several research groups in the last two decades.

Comparison of different *BAALC* transcript isoforms in various tissues hint at its role in leukemogenesis: The eight exons of the *BAALC* gene are recombined into eight different isoforms by alternative splicing [29]. Six of these eight isoforms are expressed in immature leukemic blasts, which are found neither in neuroectodermal tissues nor glioblastoma tumors despite high *BAALC* expression [29]. Other than in acute leukemia and glioblastoma, high *BAALC* expression has not been detected in other cancer types, excluding the option of *BAALC* being a general marker for neoplasia [29].

Furthermore, high *BAALC* expression was found more often in AML patients with less differentiated FAB subtypes M0, M1, and M2 and less often in M4 or M5. [30]

Contrary to expectations, there has been no proof that constitutive activation of *BAALC* encourages self-renewal or proliferation in HSPC. Nevertheless, the consideration of *BAALC* promoting leukemogenesis remains, as there is scientific evidence of *BAALC* impeding myeloid differentiation in certain cases. [31]

The research group of Prof. Julia Skokowa has already found that genes that are usually expressed in early hematopoietic stem cells, such as *BAALC*, *CD34*, *HPGDS*, *NPR3*, and *CD109*, to name a few examples, were also overexpressed in the blasts of six CN/AML patients. So, to further investigate these CN/AML blasts, they were compared to CD34+CD33+ cells from the bone marrow of pre-leukemic patients. Dannenmann and Klimiankou et al. identified the

overexpression of *BAALC* as a key event in leukemogenesis downstream of *RUNX1* and *CSF3R* mutation. [32]

1.3.2. *BAALC* as a prognostic factor in AML

The understanding of the importance of abnormal gene expression in the pathogenesis and prognosis of AML, especially in cytogenetically normal AML, has led to several studies, which have shown that high *BAALC* gene expression is an independent adverse prognostic indicator in adult patients with cytogenetically normal AML. [33]

Patients with high *BAALC* expression are less likely to achieve CR and have shorter disease-free survival (DFS) and OS rates in comparison to patients with low *BAALC* expression. [30, 34]

Independent from *FLT3 ITD, NPM1, CEBPA* mutation status, and white blood cell count, high *BAALC* expression predicted poor OS. Langer et al. concluded that "patients with high *BAALC* expression were twice as likely to die as those with low *BAALC* expression" [30].

Through gene expression profiling, Langer et al. found a unique signature associated with high *BAALC* expression. The gene expression profile in those patients displayed many similarities with the gene expression profile in hematopoietic stem cells. Furthermore, genes previously associated with a poor outcome, like *CD34*, *CD133*, and *MN1*, and the multidrug resistance gene *MDR1* (*ABCB1*), were also overexpressed in patients with high *BAALC* expression. These findings are one of several proposed explanations for the poor prognosis observed in patients with high BAALC expression. [30]

A clear understanding of the role of *BAALC* in leukemogenesis has not been accomplished yet. Investigations of the *BAALC* downstream signaling pathway have been another approach to understanding the effects of *BAALC* on hematopoietic cells.

1.3.3. *BAALC* downstream pathway

Numerous signaling pathways regulate cellular functions like differentiation, proliferation, survival, and apoptosis. Mitogen-activated protein kinases (MAPK) are essential in many cell-regulating signaling pathways.

Mortia et al. found evidence that suggests that the *BAALC* protein activates such a pathway, namely the ERK signaling pathway. The results of Morita et al. indicate that *BAALC* acts as a scaffold-like molecule for the cytoplasmatic MEKK1, a MAPK kinase kinase (MAP3K) upstream ERK. They postulate that BAALC binds MEKK1 with its N-terminal region and thereby increases its kinase activity to phosphorylate ERK. They also found evidence that BAALC inhibits the reassociation of MAP kinase phosphatase 3 (MKP3), an ERK specific phosphatase that mediates deactivation of ERK and thereby sustains ERK activation.[35, 36]

Constant ERK activation leads to proliferation and a block in differentiation. Inhibition of MEKK1, therefore, could be a possible approach for treating *BAALC*^{high} AML. [36]

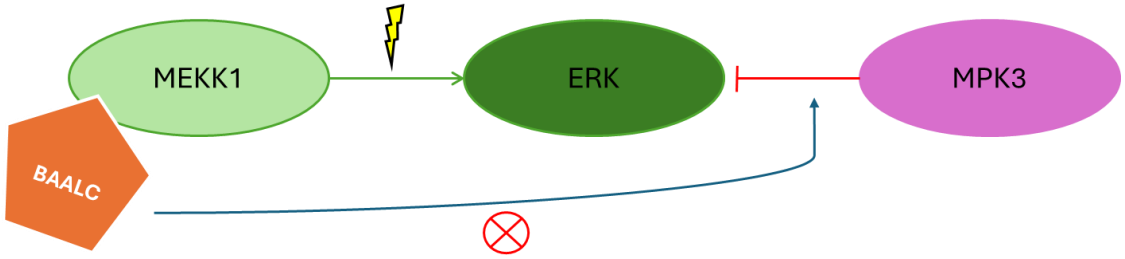

Figure 1. Hypothesized BAALC downstream pathway.
Simplified illustration of BAALC interacting in ERK signaling pathway. BAALC binds MEKK1 with its N-terminal region and thereby increases its kinase activity to phosphorylate ERK. BAALC also inhibit the reassociation of MAP kinase phosphatase 3 (MKP3) an ERK specific phosphatase (that mediates deactivation of ERK) and thereby sustaining ERK activation.

The evidence of Morita et al. suggests that the *BAALC*-induced growth advantage of leukemic blasts they observed may even rely on MEK-ERK signaling activity [35]. To intervene it this signaling pathway in *BAALC*^{high} AML, we treated cells with three different inhibitors: AZD6244, U0126, and CMPD1. These drugs were selected by Benjamin Dannenmann.

AZD6244, also known as Selumetinib, is a MEK1/2 and ERK 1/2 inhibitor. Since 2020, Selumetinib is used as an oral treatment for children with inoperable

Neurofibromatosis type 1 [37]. U0126 is a dual MEK1 and MEK2 inhibitor [38]. As a further option for a therapeutic approach for BAALChigh AML, we chose CMPD1, a non-ATP-competitive, selective inhibitor of the p38α-mediated M2Ka phosphorylation. CMPD1 was identified by Benjamin Dannenmann through a connectivity map analysis from RNA-sequencing data by comparing genes between CN/AML and CN/AML *BAALC* KO HSPCs [32]. Drug candidates were assessed by introducing a gene expression profile similar to *BAALC* KO. “A selective inhibitor of p38a-mediated MK2a phosphorylation, CMPD1, was the first hit” [32].

1.4. Aim of the study

This study aimed to investigate the role of BAALC overexpression on leukemogenesis and the behavior of leukemic blasts *in vitro* and *in vivo*.

Via CRISPR/Cas9, we planned to establish a *BAALC* knockout (KO) in *BAALC*^{high} de novo AML blasts and later *BAALC*^{high} CN/AML blasts to then compare the proliferation rate of *BAALC* KO and *BAALC* wild type (WT) cells *in vitro*.

For the *in vivo* analysis, we aimed to investigate the engraftment capacity of AML cells with and without *BAALC* knockout in NSG mice and zebrafish embryos.

In search of treatment options for patients with *BAALC*^{high} AML, we conducted experiments with three different drugs, which were selected to intervene in the signal cascade downstream of *BAALC*: CMPD1, an M2Ka inhibitor, and the MEK1 and MEK2-inhibitors U0126 and AZD6244.

The results of our research pursue a better understanding of the role of *BAALC* in leukemogenesis and to contribute to the development of new therapeutic approaches in the treatment of *BAALC*^{high} AML.

2. Probands, materials, and methods

2.1. Cell lines

Table 4: CELL LINES

Cell line	Cell type/catalog number:	Media	Company, headquarters, country
HEK 293T	embryonal kidney/ ACC 635	Complete DMEM GlutaMAX + 10 % FCS)	DSMZ, Braunscheig, Germany
K562	chronic myeloid leukemia in blast crisis/ ACC 10	Complete RPMI 1640 media + 10 % FCS	DSMZ, Braunscheig, Germany
Kasumi-1	acute myeloid leukemia/ ACC 220	Complete RPMI 1640 media + 20 % FCS	DSMZ, Braunscheig, Germany
Kasumi-6	acute myeloid leukemia/ ACC 686	Complete RPMI 1640 media + 20 % FCS	DSMZ, Braunscheig, Germany
KG-1	acute myeloid leukemia/ ACC 14	Complete RPMI 1640 media + 10 % FCS	DSMZ, Braunscheig, Germany
KG-1a	acute myeloid leukemia/ ACC 421	Complete RPMI 1640 media + 20 % FCS	DSMZ, Braunscheig, Germany
Molm 13	acute myeloid leukemia/ ACC 554	Complete RPMI 1640 media + 10 % FCS	DSMZ, Braunscheig, Germany
Sl/S (IL-3, SCF)	stromal cell line (mouse strain) / #00302	HLTM complete (see table 7)	Stemcell Technologies, Vancouver, Canada
U-937	histiocytic lymphoma/ ACC 5	Complete RPMI 1640 media + 10 % FCS	DSMZ, Braunscheig, Germany

2.2. Patient-derived primary leukemia and healthy donor cells

The patient-derived primary leukemia and the healthy donor (HD) cells were obtained from the University Children's Hospital Tübingen and the Department of Internal Medicine of the University Hospital Tübingen with the informed consent and Institutional Review Board approval of the University Hospital Tübingen (#041/2017B02; 368/2015B02).

TABLE 5: PATIENT-DERIVED PRIMARY LEUKEMIA CELLS

Anonymous Patient ID	Cell type	Media
#1273	Pediatric acute myeloid leukemia	HLTM complete with high cytokine mix (see table 7)
#1275	Pediatric acute myeloid leukemia	HLTM complete with high cytokine mix (see table 7)
#1291	Pediatric acute myeloid leukemia	HLTM complete with high cytokine mix (see table 7)
CN/AML P4	AML M2 Mutations: *GPT1; K83Q* (*RUNX1* mutation),*Q720X* (*CSF3R* mutation)	HLTM complete with high cytokine mix (see table 7)
HD2	Healthy donor	HLTM complete with high cytokine mix (see table 7)
HD64	Healthy donor	HLTM complete with high cytokine mix (see table 7)
LPH27	Healthy donor	HLTM complete with high cytokine mix (see table 7)
P12K	Pediatric acute myeloid leukemia	HLTM complete with high cytokine mix (see table 7)
P49S	Pediatric acute myeloid leukemia, FAB M5	HLTM complete with high cytokine mix (see table 7)
P84D	Pediatric acute myeloid leukemia, FAB M2	HLTM complete with high cytokine mix (see table 7)
P93A	Pediatric acute myeloid leukemia	HLTM complete with high cytokine mix (see table 7)

2.3. NSG mice

The NSG mice were obtained from The Jackson Laboratory (Bar Harbor, USA) and maintained under specific pathogen-free conditions in the research animal facility of the University of Tübingen, Germany, according to German federal and state regulations (Regierungspräsidium Tübingen, K4/13, K4/15 and §10a, 1.10.2012). The use of NSG mice for the experiments was conducted with the informed consent and Institutional Review Board approval of the University Hospital Tübingen (#041/2017B02; 368/2015B02).

2.4. Zebrafish embryos

Zebrafish lines were maintained according to standard protocols and handled following the European Union animal protection Directive 2010/63/EU and approved by the local government (Tierschutzgesetz §11, Abs. 1, Nr. 1, husbandry permit 35/9185.46/Uni TÜ). All experiments described in the present study were conducted on embryos younger than two days post-fertilization. In this study, we used a zebrafish wild type TE strain.

2.5. Materials

2.5.1. Cell culture media, sera, supplements

TABLE 6: CELL CULTURE MEDIA, SERA, SUPPLEMENTS

Medium/serum/supplement for cell culture	Company, headquarters, country
DMEM GlutaMAX™	Thermo Fisher Scientific, Waltham, USA
Fetal bovine serum (FCS) in-activated	Sigma-Aldrich, Saint Louis, MO, USA
HEPES buffer (1M)	Sigma-Aldrich, Saint Louis, MO, USA
HLTM (MyeloCult H5100)	Stemcell Technologies, Vancouver, Canada
Opti-MEM® I Reduced Serum Medium	Thermo Fisher Scientific, Waltham, USA
Penicillin/Streptomycin	Biochrom AG, Berlin, Germany
RPMI 1640	Thermo Fisher Scientific, Waltham, USA
Stem Line Medium II	Sigma-Aldrich, Saint Louis, MO, USA

2.5.2. Media and buffers

TABLE 7: MEDIA AND BUFFERS

Medium/buffer	Composition
Blocking buffer	5% SlimFast in TBS
Complete Dulbecco's Modified Ea-gle Medium (DMEM) GlutaMAX me-dium	DMEM GlutaMAX medium 10 % FCS 100 U/ml Penicillin 100 U/ml Streptomycin
Complete RPMI 1640 medium	RPMI 1640 medium 20 % FCS or 10 % FCS (depending on cell line) 100 U/ml Penicillin 100 U/ml Streptomycin

Complete Stem Line Medium II	Stem line medium II 10 % FCS 100 U/ml Penicillin 100 U/ml Streptomycin
E3 media	For 500 mL: 8,6g NaCl 0,4g KCl 1,45g $CaCl_2$ x H_2O 2,45g $MgSO_4$ x $7H_2O$ 400 mL dH_2O 2 to 5 µL NaOH Add dH_2O to the total volume of 500mL
FACS buffer	PBS 2 % FCS 1% Penicillin 1% Streptomycin
Freezing medium	90 % FCS 10 % DMSO
HLTM complete	HLTM medium 1% hydrocortisone 10^-4 1% Penicillin 1% Streptomycin
HLTM complete with high cytokine mix	HLTM medium 1% hydrocortisone 10^-4 1% Penicillin 1% Streptomycin 100 ng/mL IL-6 300 ng/mL SCF 300 ng/mL TPO 300 ng/mL FLT3L 10 g/mL IL-3

2.5.3. Chemicals, reagents, solutions, and cytokines

TABLE 8: CHEMICALS, REAGENTS, SOLUTIONS, AND GELS

Chemical/reagent/solution/cytokine	Company, headquarters, country
0,5 % PFA FACS fixation	Sigma Aldrich, St. Louis, USA
5x Colorless GoTaq Flexi Buffer	Promega, Fitchburg, USA
5x Green GoTaq Flexi Buffer	Promega, Fitchburg, USA
6x DNA Loading Dye	Thermo Fisher Scientific, Waltham, USA
AccuGene 10x TBE Buffer	Lonza Group, Basel, Switzerland
Ampuwa® Water	Fresenius Kabi Deutschland GmbH, Bad Homburg, Germany
AZD-6244 catalogue number: #S1008	Selleckchem, Houston, USA
Bovine Serum Albumin	Sigma Aldrich, St. Louis, USA
CellTiter-Glo® Buffer	Promega, Madison, USA
CellTiter-Glo® Substrate	Promega, Madison, USA
CMPD1 catalogue number: #2186	Tocris Bioscience, Bristol, Great Britain
DMSO	Sigma Aldrich, St. Louis, USA
Ethanol absolute 100 %, AnalaR NOR-MAPUR	VWR Prolabo Chemicals, Radnor, USA
FACS Clean®	BD Biosciences, San Jose, CA, USA
FACS Flow®	BD Biosciences, San Jose, CA, USA
FACS Rinse®	BD Biosciences, San Jose, CA, USA
Ficoll Paque Plus	GE Healthcare, Chicago, USA
FLT3L	BioLegend, San Diego, CA, USA

GCSF 10 µg	Stemcell Technologies, Vancouver, Canada
GelRed Nucleic Acid Gel Stain	Biotium, Hayward, USA
Hydrocortisone	Stemcell Technologies, Vancouver, Canada
IL15 (10 µg/ml)	Miltenyi Biotec, Bergisch Gladbach, Germany
IL-3	Peprotech, Cranbury, USA
IL-6	Peprotech, Cranbury, USA
IL7 (10 µg/ml)	Miltenyi Biotec, Bergisch Gladbach, Germany
Light Cycler 480 SYBR Green I Master	Roche, Basel, Switzerland
Methylene blue	Sigma-Aldrich, Saint Louis, MO, USA
MgCl2 25mM	Promega, Fitchburg, USA
PCR Nucleotide Mix	Roche, Basel, Switzerland
Phosphate buffered saline (PBS)	Thermo Fisher Scientific, Waltham, USA
Random Hexamer Primer (SO142)	Thermo Fisher Scientific, Waltham, USA
RLT buffer (RNeasy Lysis Buffer)	Qiagen, Hilden, Germany
RNase-Free DNase Set	Qiagen, Hilden, Germany
RNase-Free Water	Qiagen, Hilden, Germany
SCF	Peprotech, Cranbury, USA
TPO	Peprotech, Cranbury, USA
Trypan blue	Sigma-Aldrich, Saint Louis, MO, USA
U0126 catalogue number: #S1102	Selleckchem, Houston, USA

2.5.4. Reaction Kits

TABLE 9: REACTION KITS

Reaction Kit	Manufacturer
CellTrace™ CFSE Cell Proliferation Kit catalogue number: C34570	Thermo Scientific, Waltham, USA
LightCycler® 480 SYBR Green I Master Kit, catalogue number: 04887352001	F. Hoffmann-La Roche AG, Basel, Switzerland
MinElute PCR Purification Kit (50), catalogue number: 28004	Qiagen, Hilden, Germany
Omniscript Reverse Transcription (RT) Kit (200), catalog number: 205113	Qiagen, Hilden, Germany
P3 Primary Cell 4D-Nucleofector® X Kit catalogue number: V4XP-3032	Lonza Group, Basel, Switzerland
QIAamp DNA Micro Kit, catalogue number: 56304	Qiagen, Hilden, Germany
Qubit dsDNA HS Assay Kit catalogue number: Q33230	Thermo Scientific, Waltham, USA
RNeasy Micro Kit (50), catalogue number: 74004	Qiagen, Hilden, Germany
RNeasy Mini Kit (50), catalogue number: 74104	Qiagen, Hilden, Germany

2.5.5. Antibodies

TABLE 10: ANTIBODIES FOR FACS

Antibody	Isotype	Manufacturer
Anti-human CD11b APC Cy7	Mouse IgG1, κ	BD Biosciences, New Jersey, USA
Anti-human CD14 FITC	Mouse IgG1, κ	BD Biosciences, New Jersey, USA
Anti-human CD15 PE	Mouse IgG1, κ	BD Biosciences, New Jersey, USA
Anti-human CD16 APC	Mouse IgG1, κ	BD Biosciences, New Jersey, USA
Anti-human CD33 BV421	Mouse IgG1, κ	BioLegend, San Diego, CA, USA
Anti-human CD34 PE-Cy7	Mouse IgG1, κ	BioLegend, San Diego, CA, USA
Anti-human CD45 PE-Cy7	Mouse IgG1, κ	BioLegend, San Diego, CA, USA
Anti-human CD45 BV510	Mouse IgG1, κ	BioLegend, San Diego, CA, USA
Anti-mouse CD45 FITC	Rat IgG2b, κ	BioLegend, San Diego, CA, USA

The working concentration of each antibody for *in vitro* experiments was 100 ng/ml. For mouse experiments, see below.

2.5.6. Primer

All primers were synthetized by Eurofins, Ebersberg, Germany.

TABLE 11: PRIMERS USED FOR QPCR

Primer name	Primer sequence (5’ 3’)
h beta-actin_qF	TTCCTGGGCATGGAGTC
h beta-actin_qR	CAGGTCTTTGCGGATGTC

TABLE 12: PRIMERS USED FOR PCR

Primer name	Primer sequence (5’ 3’)
BAALC_exon1_F	GAGACTCGGAACGGTAATGCC
BAALC_exon 1_R	CCACTTACCCGAGTGCAG

TABLE 13: PRIMERS USED FOR REVERSE TRANSCRIPTION

Primer	Company, headquarter, country
Oligo-dT(18)-Primer 100 µM	Thermo Scientific, Waltham, USA
Random Primer Hexamer 100 µM	Thermo Scientific, Waltham, USA

2.5.7. Guide RNA used for CRISPR/Cas9 gene editing

TABLE 14: GUIDE RNA USED FOR CRISPR/CAS9 GENE EDITING

sgRNA name	sequence	Company, headquarter, country
BAALC p.14	GTCCAGCTCTCGTAGTAGCG	Integrated DNA Technologies, Coralville, Iowa, USA

2.5.8. Enzyme

TABLE 15: ENZYME

Enzyme	Company, headquarter, country
Go Taq Hot Start Polymerase	Promega, Fitchburg, USA
Pronase	Roche, Basel, Schweiz

2.5.9. Molecular weight standards

TABLE 16: MOLECULAR WEIGHT STANDARDS

Molecular weight standard	Company, headquarter, country
Gene Ruler 100 bp DNA Ladder	Thermo Scientific, Waltham, USA
Gene Ruler 1 kb DNA Ladder	Thermo Scientific, Waltham, USA
Quick-Loading 1 kb DNA Ladder	New England Biolabs, Hitchin, UK

2.5.10. Consumables

TABLE 17: CONSUMABLES

Consumable	Company, headquarter, country
Biosphere plus Filter Tips	Sarstedt, Nümbrecht, Germany
BD Plastipak™ 1 ml single syringe with cannula 45 x 12,7 mm (26 G)	BD Biosciences, San Jose, CA, USA
Cell strainer 45 µM	BD Biosciences, San Jose, CA, USA
Cryopreservation tubes	Corning GmbH, Kaiserslautern, Germany
DNA LoBind Tube 0.5, 1.5 ml	Eppendorf, Hamburg, Germany
Falcon tube 15, 50 ml	Sarstedt, Nümbrecht, Germany
Filter Tip Ultrapoint TipOne	Starlab, Hamburg, Germany
Filter Tips Safeguard	Peqlab, Erlangen, Germany

Light Cycler plate with adhesive seal (96 wells)	Sarstedt, Nümbrecht, Germany
Microplate, PS, 96 well, F-Bottom (chimney well), white, lumitrac	Greiner Bio-One, Kremsmuenster, Austria
PCR tubes 0.2 ml	Starlab, Hamburg, Germany
Petri dish 35x10	Greiner Bio-One, Kremsmuenster, Austria
Petri Dish 94x16	Greiner Bio-One, Kremsmuenster, Austria
Polystyrene Round-Bottom Tube	Thermo Fisher Scientific, Waltham, USA
Qubit assay tubes	Life Technologies, Carlsbad, USA

2.5.11. Equipment

TABLE 18: EQUIPMENT

Equipment	Company, headquarter, country
Automatic Flake-Ice-Machine (AF 100 AS)	Scotsman, Vernon Hills, USA
Clean bench HERAsafe	Heraeus Holding GmbH, Hanau, Germany
Centrifuge 5424	Eppendorf, Hamburg, Germany
Crystal eight Micro Centrifuge	LMS, Brigachtal, Germany
Erlenmeyer flasks	Th. Geyer, Erlangen, Germany
FACSCanto II Flow Cytometer	BD, Franklin Lakes, USA
Fluorometer (Qubit 2.0)	Life Technologies, Carlsbad, USA
Gel electrophoresis equipment (Wide Mini-Sub Cell GT Complete Systems) Hoods: - Safety Workbench LaminAir HB 2448 - Hood Biowizard Golden Line - Air Clean 600 PCR Workstation	Bio-Rad, Hercules, USA Heraeus, Hanau, Germany Kojair, Vilppula, Finland Starlab, Hamburg, Germany Biosan, Riga, Latvia

- DNA/RNA UV-Cleaner UVC/T-AR	
GloMax Multimode Microplate Reader	Promega, Madison, USA
Incubator (Kelvitron T)	Heraeus, Hanau, Germany
Light Cycler 480 (96-well version)	Roche, Basel, Switzerland
Megafuge 1.0 R	Heraeus, Hanau, Germany
Microscope (Laborlux S)	Leitz, Wetzlar, Germany
Microplate shaker	Thermo Fisher Scientific, Waltham, USA
Microwave (Micromat 15-w)	AEG, Nuremberg, Germany
Mouse injection cage type B 32 mm 100680	G&P Kunststofftechnik, Kassel, Germany
Mouse injection cage type C 25 mm 100690	G&P Kunststofftechnik, Kassel, Germany
Neubauer C-Chip counting chamber	Sigma-Aldrich, Saint Louis, MO, USA
Pipettes: - Pipetus 100-240 V - Reference variable - Research plus variable - Serological pipette 5, 10, 25 ml - Transfer pipette	 Hirschmann, Eberstadt, Germany Eppendorf, Hamburg, Germany Eppendorf, Hamburg, Germany Sarstedt, Nümbrecht, Germany Sarstedt, Nümbrecht, Germany
Refrigerators	Liebherr, Bulle, Switzerland
Thermocycler (Mastercycler nexus GX2)	Eppendorf, Hamburg, Germany
Thermomixer compact	Eppendorf, Hamburg, Germany
UV transilluminator (Gel iX Imager)	Intas Science Imaging, Göttingen, Germany
Vortex mixer (Genius 3)	IKA, Staufen, Germany

2.5.12. Softwares

TABLE 19: SOFTWARES

Software	Company, headquarter, country
FACSCanto II Software	BD Biosciences, Franklin Lakes, USA
FACSDiva	BD Biosciences, Franklin Lakes, USA
FlowJo	Tree Star, Ashland, USA
GraphPad Prism 8	GraphPad, San Diego, USA
ICE Analysis	Synthego, Silicon Valley, USA
LightCycler 480 Software release 1.5.0	Roche, Basel, Switzerland
Microsoft Word 2016 for Windows 10 Microsoft Excel 2016 for Windows 10 Microsoft PowerPoint 2016 for Windows 10	Microsoft, Redmond, USA
NanoDrop 2000 Software	Thermo Fisher Scientific, Waltham, USA

2.6. Methods

2.6.1. Isolation of MNCs from bone marrow samples

The mononuclear cells (MNCs) were isolated from the bone marrow samples through a density gradient centrifugation.

The samples were diluted in a 1:2 ratio with PBS buffer, carefully plated on Ficoll-Plaque Plus, and afterward centrifuged (RT, 25 min, 500g, no brake, no acceleration). The following steps were performed on ice. The interphase was isolated and washed twice by adding 30 ml PBS (4°C) buffer and centrifuging (8°C, 8 min, 340g), removing the supernatant, and resuspending the pellet with another 30 ml PBS (4°C) and repeating the centrifugation. After removing the supernatant the second time, the cell pellet was resuspended in 1-5 ml PBS. 10µL cell suspension was used for a cell count. The suspension was diluted in a 1:10 ratio with 3% acetic acid methylene blue and then counted using a Neubauer chamber. Depending on the material of interest (DNA, RNA, or proteins), the cells were lysed through the respective solution. Freezing media (DMSO and FCS, 1:10) was added before the cells were frozen at -20°C or -80°C.

2.6.2. Manual cell count

The number of vital cells was determined by manual cell count using Neubauer counting chambers and trypan blue. Trypan blue stains dead cells, which can then be excluded, allowing the count of only vital cells. The following calculation was used to estimate the cell number per milliliter:

$$\text{number of cells per ml: } = \frac{\text{number of counted cells}}{\text{number of counted squares}} \times \text{dilution factor} \times 10^4$$

2.6.3 Drug treatment

To analyze the impact of high *BAALC* expression on the cell viability of AML cells, we treated cells with three different inhibitors: AZD6244, CMPD1, and U0126. These inhibitors were chosen because of their interference in the cell pathway downstream of *BAALC*. AZD6244, also known as Selumetinib, is a MEK1/2 and ERK 1/2 inhibitor. CMPD1, a non-ATP-competitive, is a selective inhibitor of p38α-mediated MK2a phosphorylation. U0126 is a dual MEK1 and MEK2 inhibitor. The treatment was first performed on the cell line Kasumi-1, which is characterized as a *BAALC*^{high} cell line [39].

Furthermore, the drugs were tested on de novo AML patients P84D, P49S, and P12K, which were also *BAALC*^{high} expressing cells. The treatment was executed in 3 different concentrations (1µM, 2µM or 5µM for CMPD1 and AZD6244 and 1µM, 5µM or 10 µM for U0126) and analyzed in comparison to a healthy donor LPH27. The Cell viability was measured after four days of treatment via CellTiter-Glo® Luminescent Cell Viability Assay.

2.6.4 CellTiter-Glo Luminescent Cell Viability Assay

The cell viability of cells treated with different drugs was measured via the CellTiter-Glo Luminescent Cell Viability Assay. To prepare the reagent, the CellTiter-Glo® Buffer had to be thawed and stored at RT up to 48 hours before use. Before its use, the lyophilized CellTiter-Glo® Substrate had also been equilibrated to RT. The CellTiter-Glo® Buffer was added to the CellTiter-Glo® Substrate. This formed the CellTiter-Glo® Reagent. The solution was then homogenized by vortexing.

The cells were seeded four days before the analysis in a concentration of 0.5x 10^6 cells/ml with 100 µl per well in a 96-well Microplate (lumitrac). The plate was equilibrated at RT for 30 minutes before adding 100 µl of the CellTiter-Glo® Reagent to each well. The plate was then mixed on a plate shaker for 2 minutes to induce cell lysis. The plate was then incubated at RT for another 10 minutes to stabilize the luminescent signal. The luminescence was recorded by a GloMax Multimode Microplate Reader. The data was then analyzed using Microsoft Excel.

2.6.5 Electroporation

Through the transfection with chemically modified single guide RNA (sgRNA), we aimed to achieve a knockout of the *BAALC* gene. We used the P3 Primary Cell 4D-Nucleofector® X Kit (Lonza, Switzerland) and modified the Amaxa™ 4D-Nucleofector™ Protocol for unstimulated Human $CD34^+$ Cells. After the initial cell count, the ribonucleoprotein (RNP) complex was prepared. For 1x10^6 cells we used 3.3 µl sgRNA (8µg/µL) and 2 µl Cas9 (15µg/µL). The RNP complex was then incubated at RT for 20 min. The cells were centrifuged (RT, 5 min, 100 g) and washed once with PBS. To prepare the nucleofection solution, 18 µl supplement was added to 82 µl Nucfection solution. The cell pellet was resuspended in the 100 µl Nucleofection solution and pipetted into a big cuvette. The electroporation program was chosen based on prior experiments, testing the viability of the cells after electroporation with a mock sgRNA. For the AML primary cells, we used the programs with the highest cell viability: CA-137, CM-138, and DS-138. The cuvettes were incubated for 15 min at 37 °C after electroporation. Prewarmed medium was added to the cells. The cells were then transferred to a plate. To assess the success of the electroporation and the knockout, we took approximately 1x10^5 cells after two and after ten days, isolated the DNA, and performed sanger sequencing analysis (see chapter 2.6.11.)

2.6.6 Isolation of Genomic DNA

The isolation of genomic DNA of cells was performed pursuing the protocol for “Isolation of Genomic DNA from Small Volumes of Blood” of the QIAamp DNA Micro kit (Qiagen, USA). Instead of whole blood, the chosen number of cells (minimal 20x10^4 and maximal 2x10^6 cells) was resuspended in 30µl PBS buffer.

The concentration of the isolated DNA was finally measured by a fluorometer (see 2.5.10. Quantification of DNA products by Qubit).

2.6.7 PCR

The standard master mix used for each PCR reaction and the PCR program are shown in tables 19 and 20.

TABLE 20: PCR MASTER MIX FOR *BAALC*

Master mix	Components	Amount in µL per sample
1x	5x colorless Flexi buffer	4
	25 mM MgCl2	1
	10 mM dNTP's	0,5
	DMSO 100%	0,6
	Go Taq G2 Hot Start 5u/µl	0,2
	Forward Primer 10 pmol/µl	1 µl
	Reverse Primer 10 pmol/µl	1 µl
	ddH_2O	10,2 µl
	Template	1,5 µl
	Total volume	**20 µl**

TABLE 21: PCR PROGRAM FOR *BAALC* USING THERMOCYCLER

PCR steps	Temperature	Time	Number of Cycles
	95 °C	5 min	1x
Denaturation **Annealing** **Amplification**	95 °C 50,1 °C 72 °C	15 sec 15 sec 45 sec	35x 35x 35x
	72 °C 8 °C	5 min hold	1x hold

The PCR products were checked by gel electrophoresis.

2.6.8 Gel electrophoresis

Agarose gel was made using a 1x TBE buffer system with an agarose concentration of 1,5 %. 10 µl of GelRed was used to stain nucleic acid in the gel.

3,5 µl of samples were mixed with 1 µl of 6x DNA loading dye. By a constant voltage of -90 mV for 60 min, the gel electrophoresis apparatus created an electrical field across a gel matrix through which the nucleic acid fragments migrated. The distances that nucleic acid fragments migrate in a gel matrix correlates with their size, creating bands of similar sized fragments. When the run was completed, the bands were visualized by UV-transillumination.

The *BAALC* PCR samples that showed a band at around 400 to 500 bp in the gel electrophoresis were purified (see chapter 2.6.9.).

2.6.9. PCR Purification

The PCR samples were purified using the MinElute PCR Purification Kit (50) (Qiagen, USA) according to the manufacturer's instructions.

The DNA concentration of the purified PCR samples was measured with a fluorometer (Qubit) (see also 2.5.10 Quantification of DNA products by Qubit).

2.6.10. Quantification of DNA by Qubit

The DNA samples were measured by a fluorometer (Qubit 2.0, Life Technologies, USA). 198 µl Qubit DNA working solution and 1 µl fluorescent DNA dye were pipetted in a Qubit assay tube and then shortly vortexed. 1 µl of the sample was added. After another short vortexing, the samples were measured by a fluorometer. The measurement was recalculated to the stock concentration.

2.6.11. Sanger sequencing analysis

Sanger sequencing was utilized to determine the percentage of indels leading to a knockout of BAALC. 20µl of the PCR product with a concentration between 5 - 50 ng/ul as well as 20 µL of the respective Primer (BAALC.gDNA.ex1.F or R) was sent to the GATC Custom DNA Sequencing Service (of Eurofins Genomics, Cologne). The results were analyzed with Synthego's ICE Analysis tool [40].

2.6.12. Total RNA purification

To assess the *BAALC* expression rate, we isolated and purified RNA of selected cell lines and AML primary patients according to the Total RNA purification protocol of the RNeasy Mini kit (Qiagen, USA). Beforehand, around 5x10^6 cells were lysed in an RLT buffer.

2.6.13. Quantification of RNA by NanoDrop

The RNA concentration and the sample's purity were analyzed by a NanoDrop spectrophotometer (Thermo Fisher Scientific, USA). For blank sample, 1,5µl of RNase-free water was used. For the measurement, 1µl of the sample was applied to the spectrophotometer.

2.6.14. cDNA synthesis

For further analysis, e.g., qPCR, the RNA was reverse-transcribed into cDNA. For this purpose, the Omniscript Reverse Transcription Kit protocol (Qiagen, USA) was used. The RNA concentration in the samples had to be in a range of 50ng and 2µg per µl. 300 ng of RNA was diluted with the according amount of ddH_2O to achieve a total amount of 27µl ddH2O-RNA mixture. Master mix 1 (see table 22) was prepared and incubated according to program 1 (see table 23). Afterward, the master mix 2 was added. Immediately after program 1 was finished, 9 µl of the master mix 2 was added to the sample and then incubated with program 2. The final cDNA was finally stored at -20 °C.

TABLE 22: REVERSE TRANSCRIPTION MASTER MIXES FOR *BAALC*

Master mix	Master mix components	Amount in µl
Master mix 1	5'-d(T)18-3' primer (10 µM)	2
	Random Hexamer Primer (10 µM)	2
	ddH_2O -RNA mixture	27
	Total volume	**31**
Master mix 2	10x RT buffer	4
	5mM dNTPs	4
	RT enzyme	1
	Total volume	**9**

TABLE 23: REVERSE TRANSCRIPTION THERMOCYCLER SETUP FOR *BAALC*

Program	Temperature	Time
Program 1	70 °C	5 min
	4 °C	1 min
Program 2	42 °C	60 min
	70 °C	10 min
	4 °C	hold

2.6.15. Real-time quantitative PCR

qPCR was used to identify level of BAALC expression and categorize cell lines and patient samples into cells with high or low *BAALC* RNA expression.

The cDNA was diluted at 1:20 with ddH_2O. β-actin was chosen as the house-keeping gene. SYBR Green I dye as the fluorescent reagent and forward and reverse primer was set up and pipetted into a LightCycler 96-well plate (see table 24). The respective cDNA was added. Gene expression was measured in triplicates. No Template Control (NTC) served as negative control. The plate was shortly centrifuged (5min, 2000rpm). Corresponding to the LightCycler 480 protocol (Roche, Switzerland), the reaction setup of program 1 (see table 25) was used. The data was interpreted using the LightCycler 480 Software (Roche, Switzerland). The results were finally analyzed with the comparative C_T ($\Delta\Delta C_T$) method [41].

TABLE 24: QPCR FOR *BAALC* MASTER MIX

Master mix	Master mix components	Amount in µl
1x	SYBR Green 10 mmol	5
	10 pmol Primer Mix (F and R primer)	0.8
	cDNA (ddH_2O for NTC)	4,2
	Total volume	**10**

TABLE 25: QPCR SETUP FOR *BAALC* USING LIGHTCYCLER

qPCR steps	Temperature	Time	Cycles
(1) Pre-incubation	95 °C	10 min	1x
(2) Amplification Denaturation Annealing Amplification	 95 °C 60 °C 72 °C	 10 sec 10 sec 30 sec	45x
(3) Melting program	95 °C 65 °C	4 sec 1 min	1x

2.6.16. Immunofluorescent staining of cell surface markers

To stain the cell surface markers, 0.1 – 1x 10^6 cells were transferred into FACS tubes and washed once with PBS buffer. The cell pellet was then resuspended in 100µL FACS buffer. A list of used fluorochrome-labeled antibodies is provided in Table 10. 2-3 µL of each antibody was added to the sample, which was then incubated at RT for 15 min. After that, cells were washed with FACS buffer and fixated with 200µL 0,5% PFA. The sample was then stored at 4°C in a dark place. All centrifugation steps were conducted at 300 *g* for 5 min.

2.6.17. FACS analysis

The cell samples were analyzed on a 14-color FACSCanto II Flow Cytometer or LSR II cytometer and evaluated using FlowJo or BD FACSDiva™ software. For every FACS analysis, vital mononuclear cells were chosen, and doublets were left out based on scatter features.

2.6.18. Xenograft zebrafish embryo model

Before the injection of AML cells into zebrafish embryos, the cells were labeled using GFP (via a CFSE labeling kit (Thermo Scientific, USA). For the staining, 1x10^6 cells per sample were prepared. The 10 mM stock CFSE reagent was diluted into a concentration of 1µM in PBS. The cells were centrifuged at 300 *g* for 5 min and resuspended in 5mL of the CFSE dilution. After incubation for 15 minutes at 37°C in the dark, the cells were washed in medium and then resuspended in prewarmed medium, followed by another 30 minutes of incubation at 37 °C. The 24-hour post-fertilization zebrafish embryos were released from their chorion by adding 500µL pronase with a concentration of 40mg/10mL to 10 mL embryo medium and incubated for 5 min at 37°C. The embryos were then washed three times in embryo medium in a beaker and then put into petri dishes with agarose gel with indentations to fixate the embryos.

The injection needles were filled with the cell suspension through a pipette. The amount of cell suspension was estimated by the diameter of the drop which shot out of the needle into mineral oil. The injection device was set at a pressure of 20 PSI and 1-5 x 100 ms pace. For the injection, the needle was inserted into the

yolk sac and then retracted. This way, the cell suspension was placed in the perivitelline space. For FACS analysis, the zebrafish embryos were washed with PBS. Five zebrafish embryos were placed on a cell strainer. After adding 500µL of FACS buffer, the fish were pestled with the stamp of a syringe. 500µL of FACS buffer was added, and then the cell suspension was transferred into an Eppendorf tube. The cell suspension was centrifuged at RT for 5 min at 300 g. The cells were transferred into FACS tubes. The percentage of CFSE-labeled cells was analyzed (see chapter 2.6.17.).

2.6.19. Xenograft mice model

For the xenograft mice model, around 5 Mio cells of KG-1a WT or *BAALC* KO cell lines and 0,5 - 1,2x 10^6 of the AML primary patient samples P84D, P12K, and P49S were intravenously injected into the tail vain of 6 weeks old NSG mice 4 hours after radiation with 225 Gy. Four weeks after the injection, peripheral blood of the mice was analyzed by FACS to assess the leukemia engraftment. Depending on the leukemia engraftment in the peripheral blood samples and the clinical signs of leukemia in the mice, the mice were euthanized between 4 and 7 weeks after injection. Bone marrow and spleen were sieved through a cell strainer, stained for FACS, and then analyzed regarding the leukemic engraftment of the AML cells with *BAALC* WT and *BAALC* KO by FACS.

2.6.20. Statistical analysis

Statistical significance of data sets was gained by 2-sided student t-test using Microsoft Excel. P-values < 0.05 were considered as statistically significant with * $p < 0.05$, ** $p < 0.01$, *** $p < 0.001$, **** $p < 0.0001$.

3. Results

3.1. Selecting *BAALC*^{high} cell lines and patient samples

We selected cell lines and AML primary patient samples for the experiments based on their *BAALC* expression determined by qPCR.

The *BAALC* mRNA expression of each AML cell line and AML primary patient sample was compared to the *BAALC* expression of two CD33+ and three CD34+ healthy donor cells (data of HD was pooled). The *BAALC* mRNA expression of all investigated cell lines was normalized to β-actin mRNA expression. β-Actin was used as an internal expression reference.

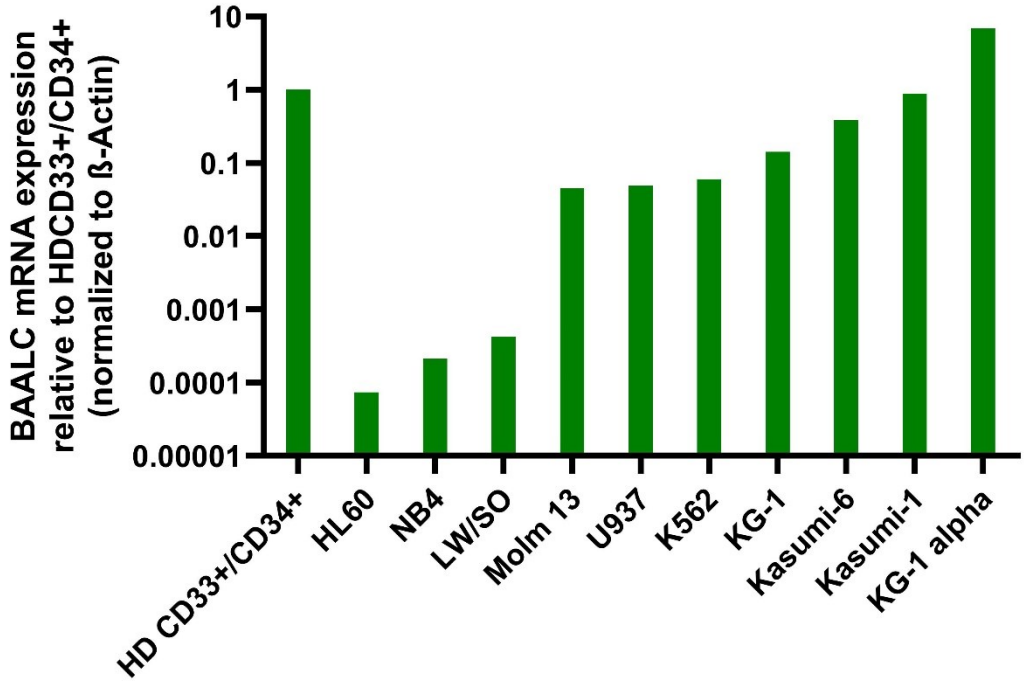

Figure 2. BAALC mRNA expression in different cell lines relative to five pooled HD HPSC (normalized to β-Actin).

Due to their relatively high *BAALC* expression, Kasumi-1 and KG-1a were selected as *BAALC*^{high} cell lines for further investigations.

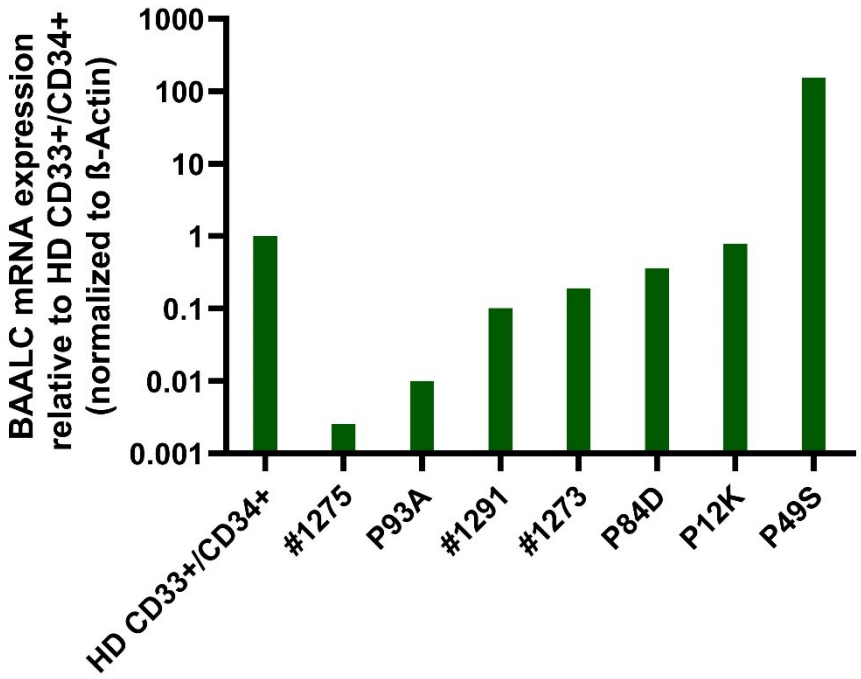

Figure 3. BAALC mRNA expression of AML primary patient samples relative to five pooled HD HPSC (normalized to β-Actin).

From the investigated AML primary patient samples, P84D, P12K, and P49S were selected as *BAALC*^{high} blasts.

3.2. Establishment of *BAALC* KO in AML primary blasts

To examine the impact of *BAALC* expression in primary AML blasts, we aimed to establish a *BAALC* knockout using CRISPR-Cas9 technology. We first tried to use a lentiviral delivery of CRISPR/Cas9 constructs to achieve an efficient *BAALC* KO. However, the amount of virus needed to gain a sufficient amount of KO cells led to a high number of cell death due to high toxicity (data not shown).

Since nucleofection of primary AML blasts with standard programs showed to be too toxic as well, we tested several electroporation programs of the Lonza Amaxa 4D-Nucleofector protocol to find programs with low toxicity. The toxicity was assessed by comparing the number of living cells three days post electroporation to the number of cells seeded (Fig. 4).

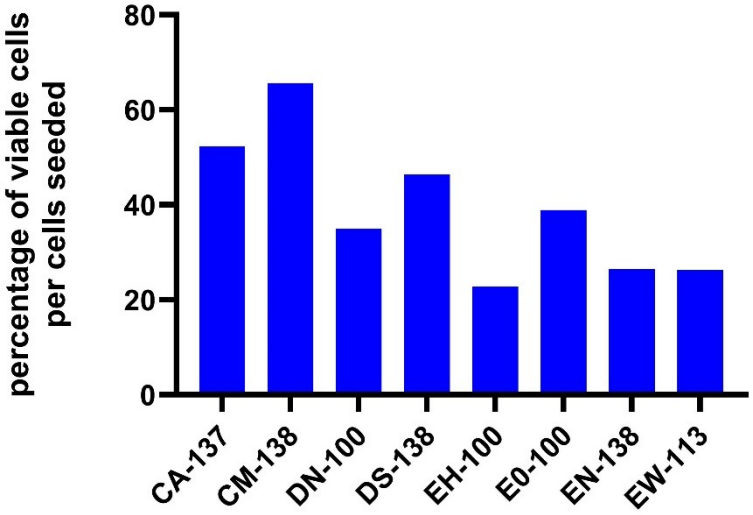

Figure 4. Effect of different electroporation programs on cell viability of AML primary blasts after 3 days.

0,4 Mio (#1273) or 0,8 Mio (P84D) cells of AML primary patient samples were electroporated using the eight shown electroporation programs. After 3 days the amount of living cells was measured via manual cell count and compared to the amount before electroporation. Data represent means from two experiments with one primary AML patient sample each (P84D and #1273).

After three days, the electroporation programs CA-137, CM-138, and DS-138 showed the most minor decrease in cell viability. Under these programs, the cell viability of primary AML patient sample P84D was even up to 80 to 100% after three days. Primary AML patient sample #1273 showed lower cell viability overall, but for both samples, the programs CA-137, CM-138, and DS-138 showed the lowest toxicity. These three programs were chosen for further experiments.

The previously selected primary AML patient samples P84D, P12K, and P49S were each electroporated with the three selected programs CA-137, CM-138, or DS-138 using CRISPR/Cas9 ribonucleoprotein (RNP) assembled with chemically modified single guide RNA (sgRNA) to knockout the *BAALC* gene.

Two days after electroporation, we isolated DNA, amplified the area of interest of the *BAALC* gene by PCR, and performed Sanger sequencing to check the results of *BAALC* gene editing. This procedure was repeated ten days post electroporation to verify the knockout was stable.

The knockout efficiency was evaluated using the ICE web tool from Synthego (https://ice.synthego.com), which provides a quantitative assessment of gene editing (see chapter 2.6.11.).

The sequencing result of each sample is shown in the following figures.

Figure description for figures 5 to 13 is found on page 60.

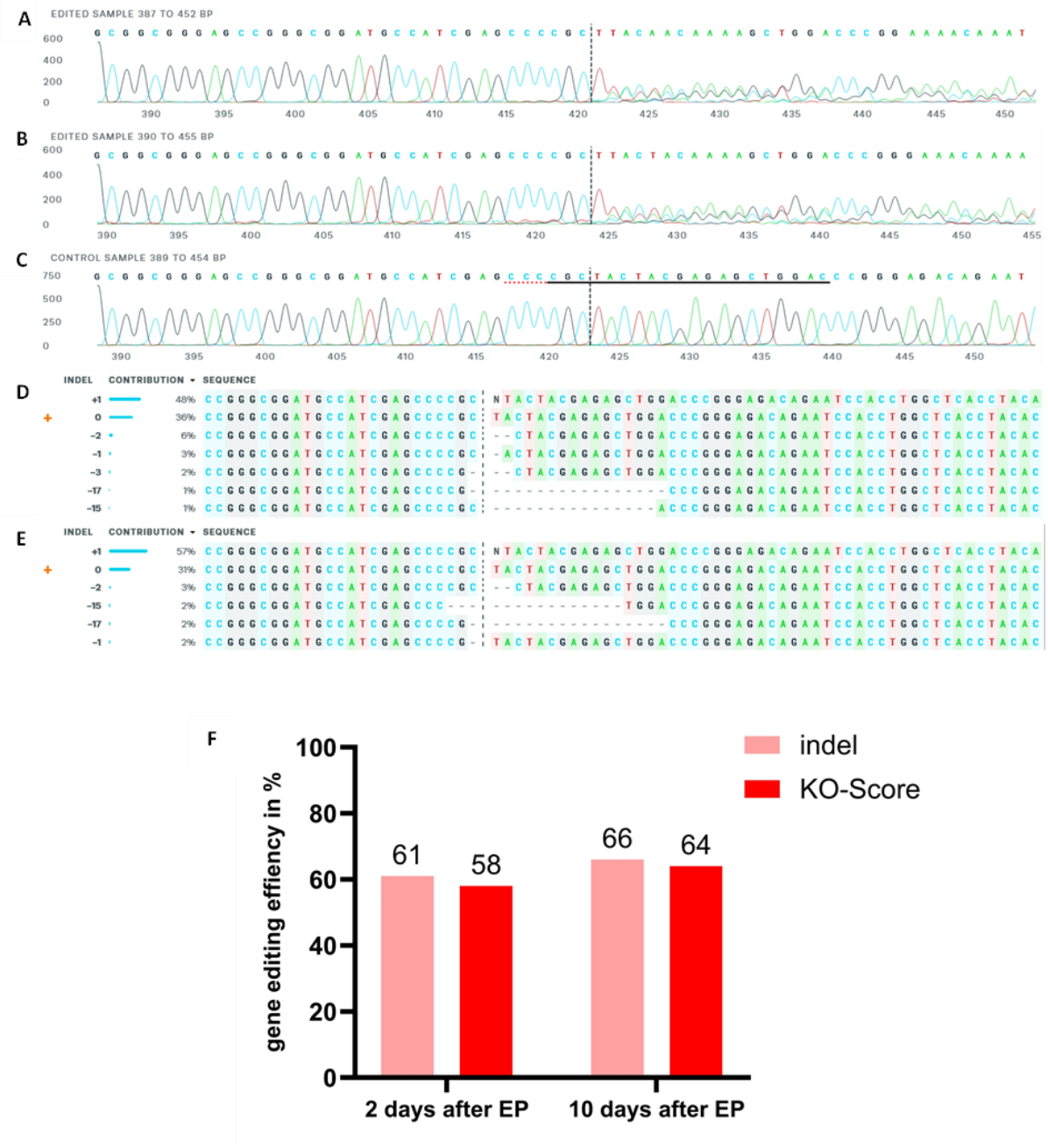

Figure 5. Analysis of AML primary sample P84D 2 and 10 days after electroporation with program CA-137.

The sequencing of the BAALC gene in AML primary patient sample P84D two days after electroporation using the program CA-137 showed a percentage of 61 successfully edited genome. Knockout was found in around 58 percent of the cells.

Ten days post-electroporation, the knockout score for this sample increased slightly to 64 percent.

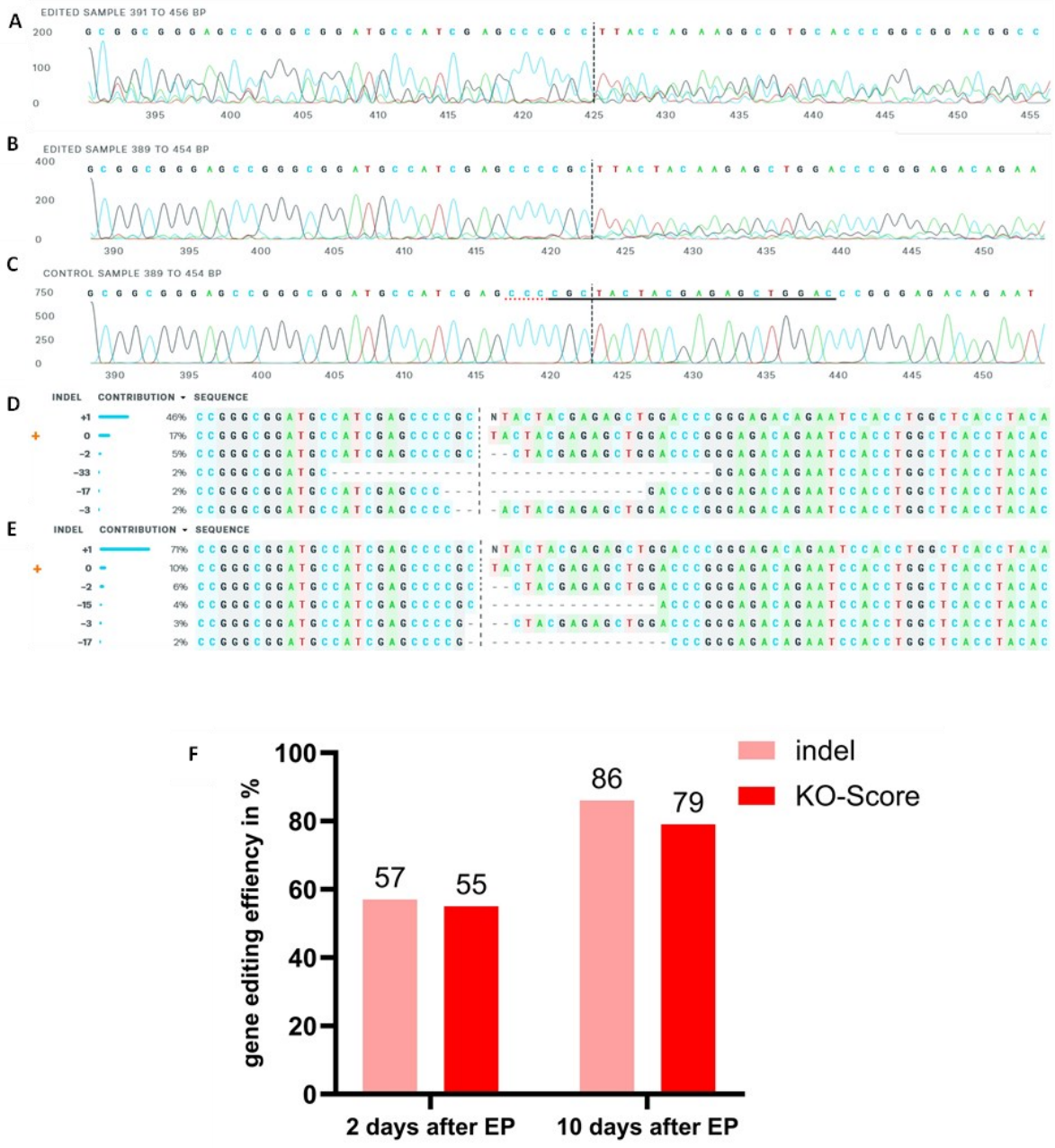

Figure 6. Analysis of AML primary sample P84D 2 and 10 after electroporation with program CM-138.

The sequencing of the *BAALC* gene in AML primary patient sample P84D two days after electroporation using the program CM-138 showed a percentage of 57 successfully edited genome. Knockout was found in around 55 percent of the cells.

Ten days post-electroporation, the knockout score increased to 79 percent.

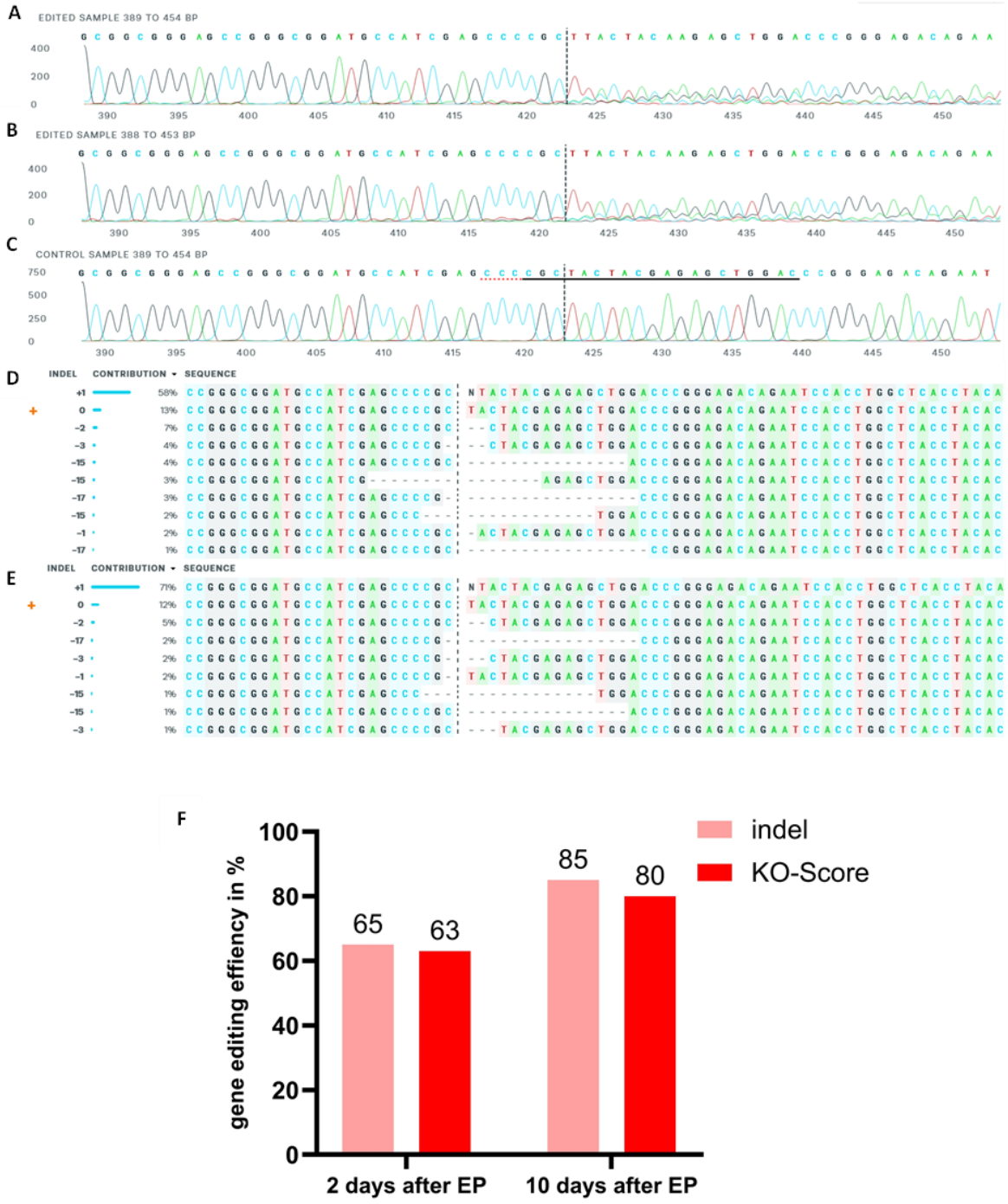

Figure 7. Analysis of AML primary sample P84D 2 and 10 days after electroporation with program DS-138.

The sequencing of the BAALC gene in AML primary patient sample P84D two days after electroporation using the program DS-138 showed a percentage of 65 successfully edited genome. Knockout was found in around 63 percent of the cells.

Ten days post-electroporation, the knockout score increased to 80 percent.

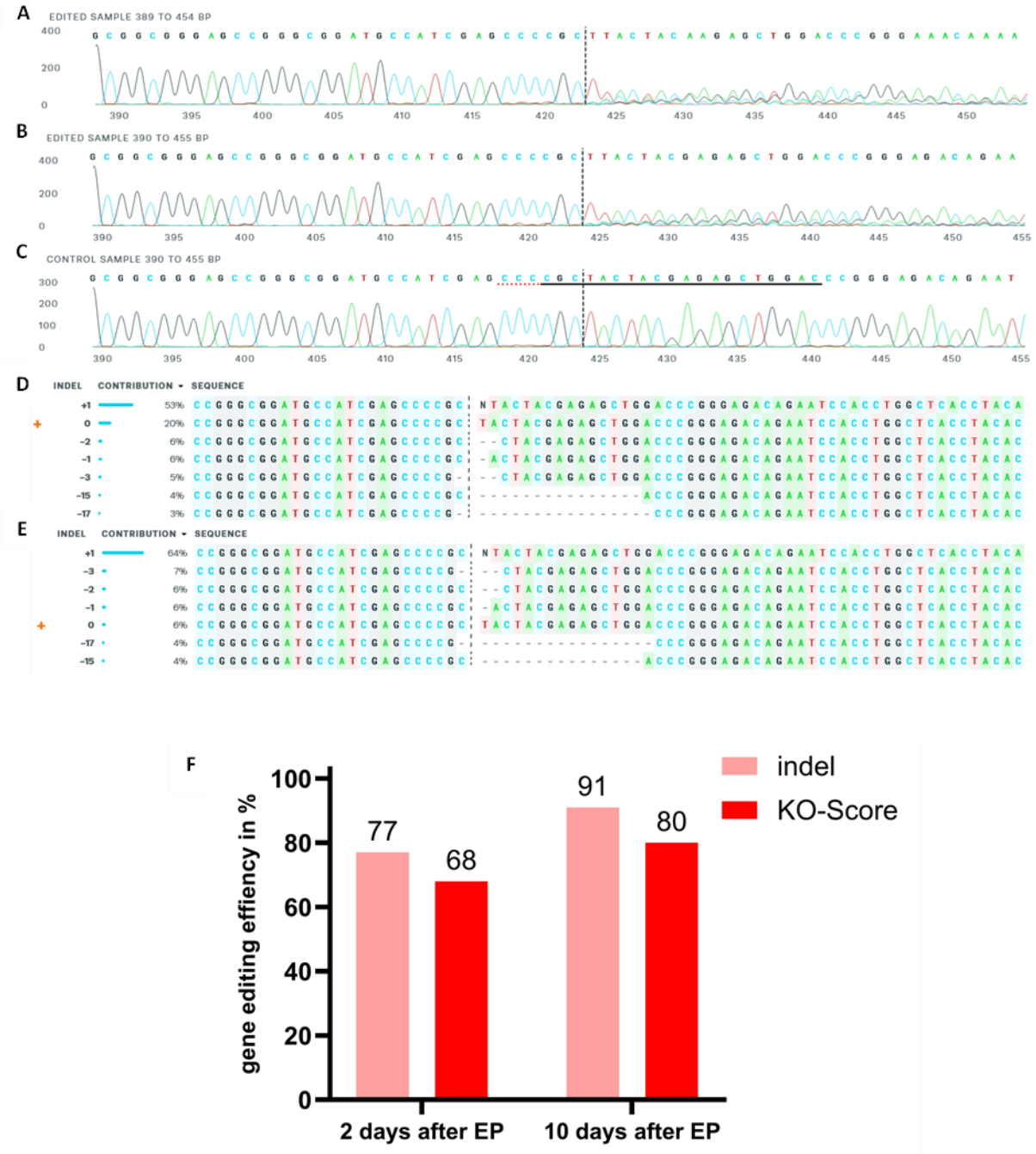

Figure 8. Analysis of AML primary sample P12K 2 and 10 days after electroporation with program CA-137.

The sequencing of the BAALC gene in AML primary patient sample P12K two days after electroporation using the program CA-137 showed a percentage of 77 successfully edited genome. Knockout was found in around 68 percent of the cells.

Ten days post-electroporation, the knockout score increased to 80 percent.

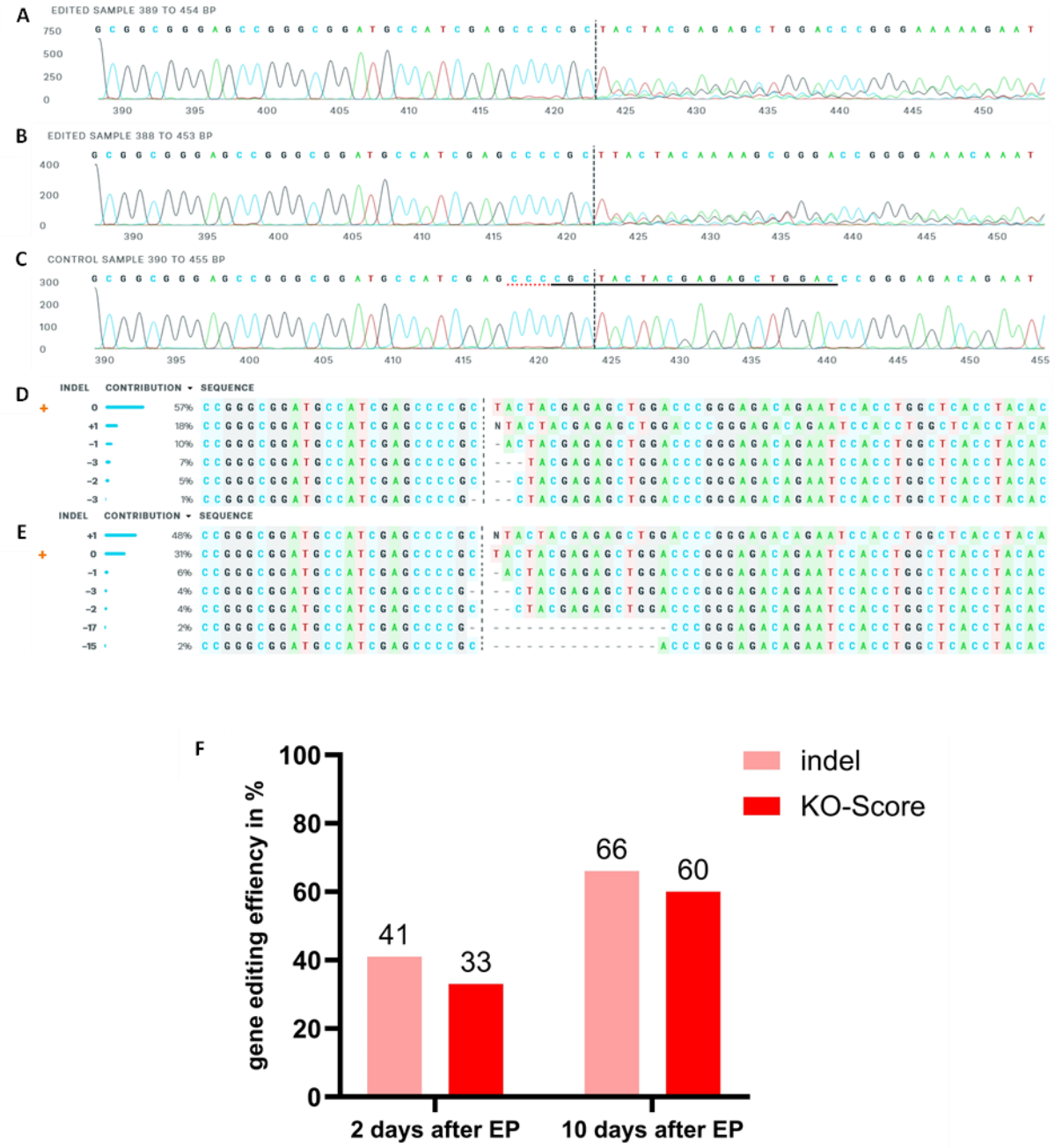

Figure 9. Analysis of AML primary sample P12K 2 and 10 days after electroporation with program CM-138.

The sequencing of the BAALC gene in AML primary patient sample P12K two days after electroporation using the program CM-138 showed a percentage of 41 successfully edited genome. Knockout was found in around 33 percent of the cells.

Ten days post-electroporation, the knockout score increased to 60 percent.

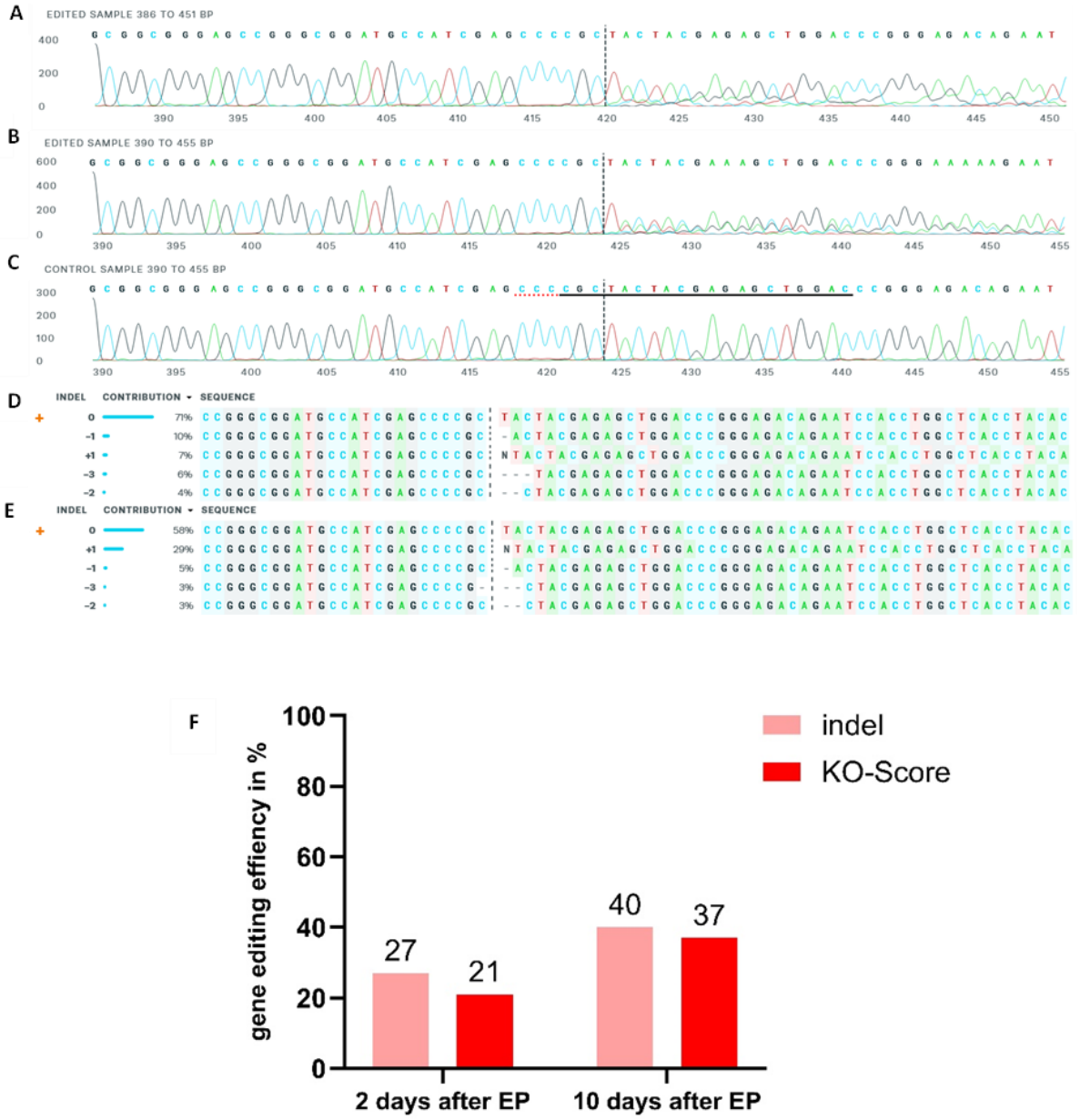

Figure 10. Analysis of AML primary sample P12K 2 and 10 days after electroporation with program DS-138.

The sequencing of the *BAALC* gene in AML primary patient sample P12K 2 days after electroporation using the program DS-138 showed a percentage of 27 successfully edited genome. Knockout was found in around 21 percent of the cells.

Ten days post-electroporation, the knockout score increased to 37 percent.

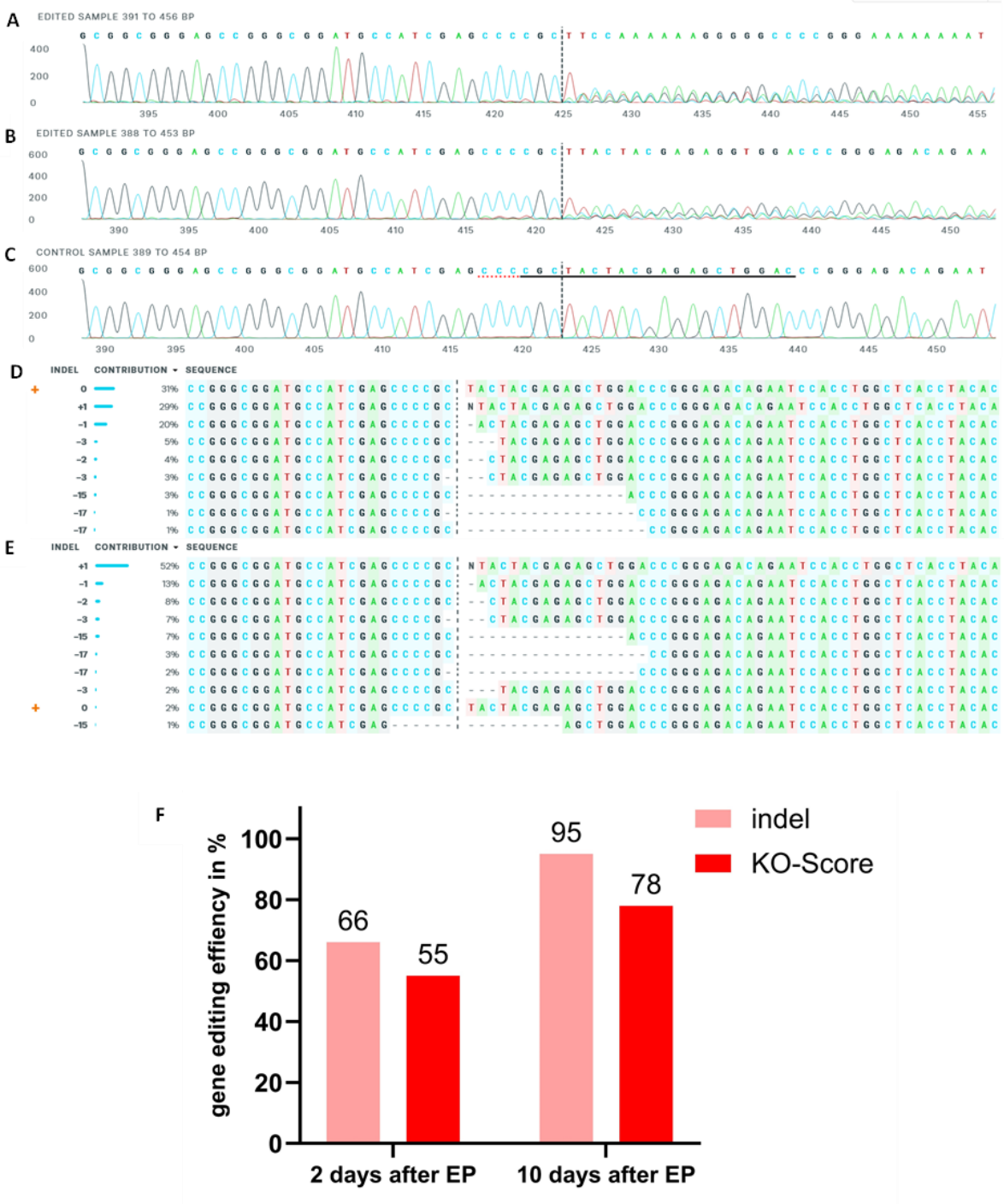

Figure 11. Analysis of AML primary sample P49S 2 and 10 days after electroporation with program CA-137.

Sequencing the BAALC gene in AML primary patient sample P49S two days after electroporation using the program CA-137 showed a percentage of 66 successfully edited genome. Knockout was found in around 55 percent of the cells.

Ten days post-electroporation, the knockout score increased to 78 percent.

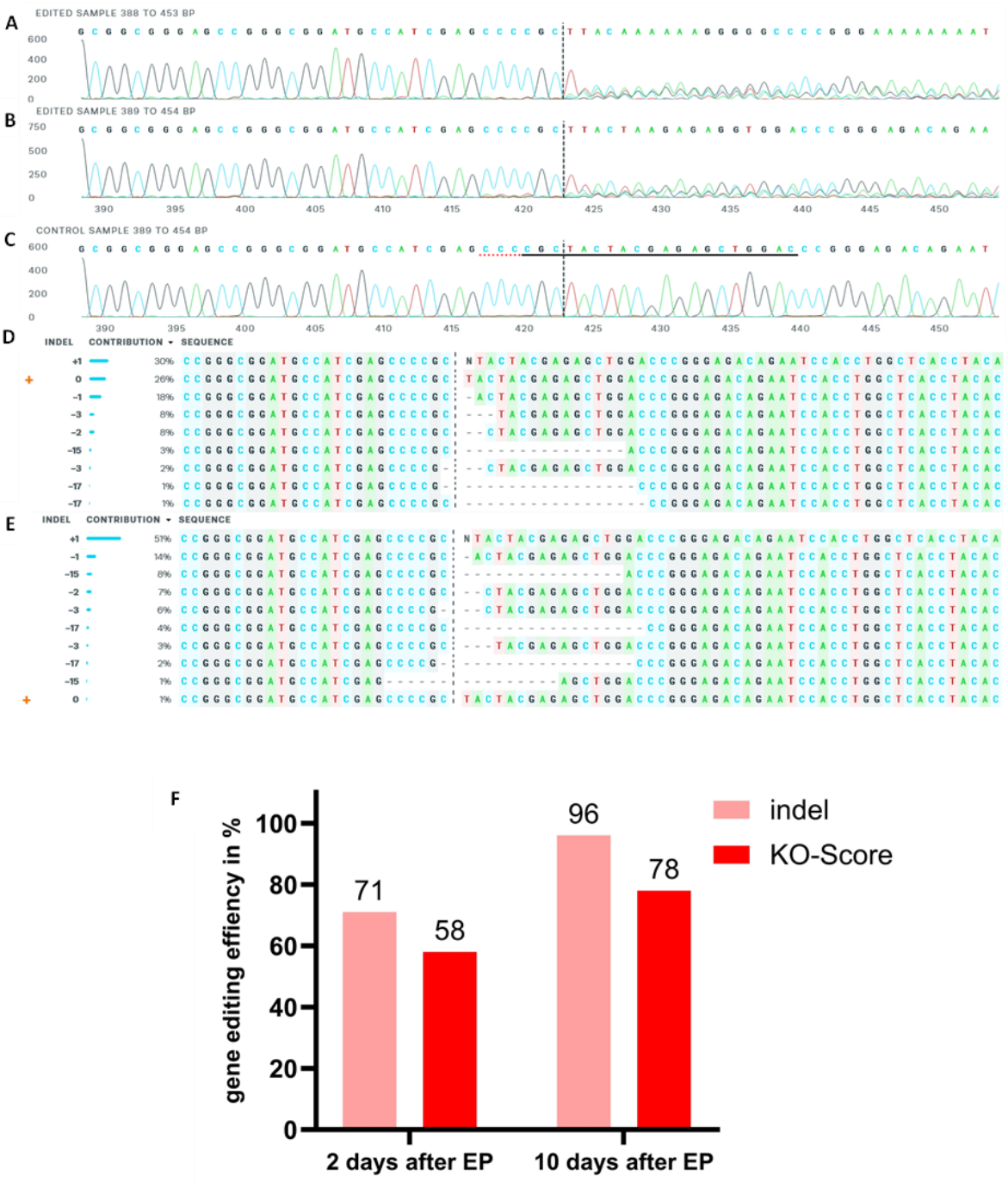

Figure 12. Analysis of AML primary sample P49S 2 and 10 days after electroporation with program CM-138.

Sequencing the *BAALC* gene in AML primary patient sample P49S two days after electroporation using the program CM-138 showed a percentage of 71 successfully edited genome. Knockout was found in around 58 percent of the cells.

Ten days post-electroporation, the knockout score increased to 78 percent.

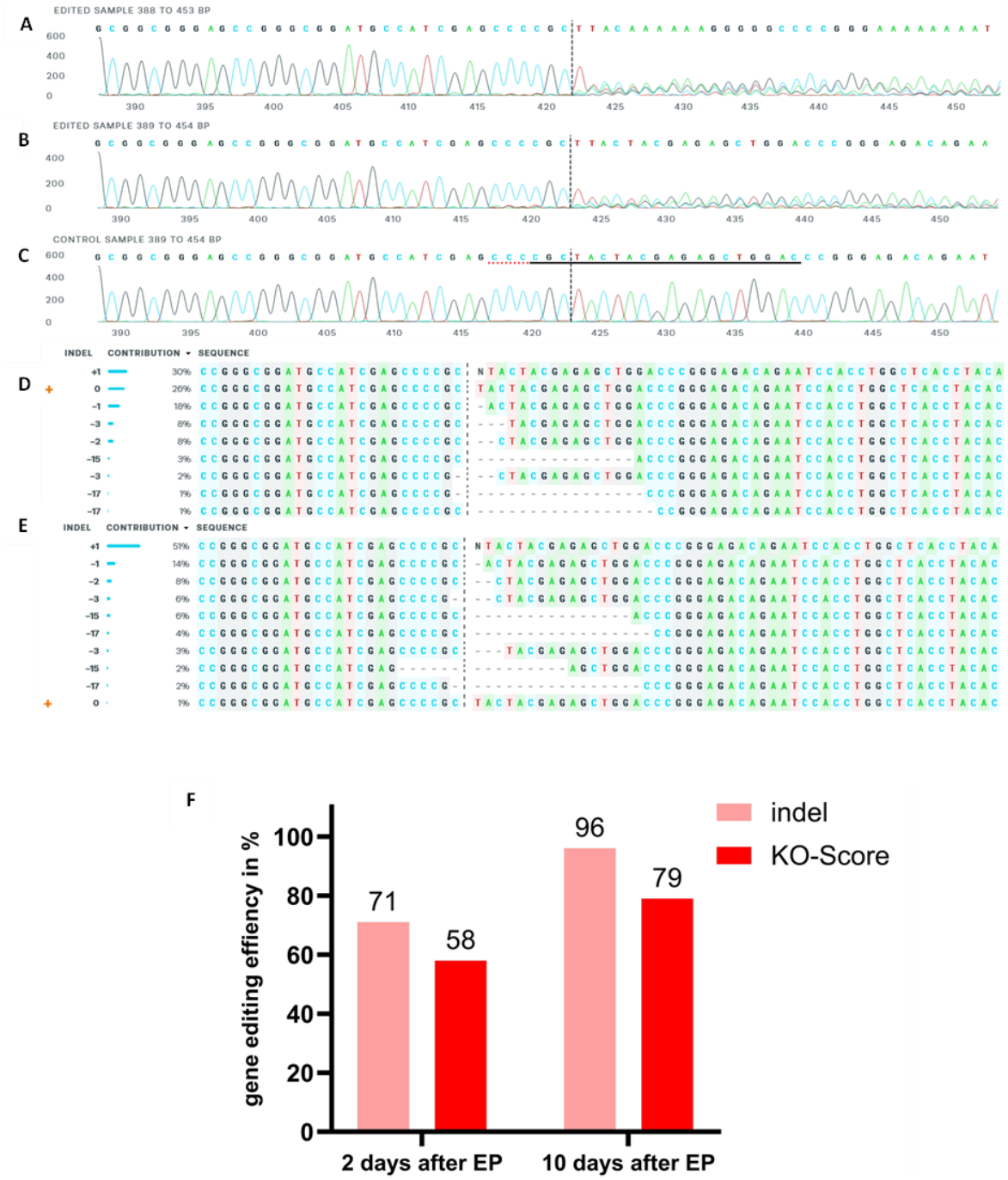

Figure 13. Analysis of AML primary sample P49S 2 days after electroporation with program DS-138.

The sequencing of the *BAALC* gene in AML primary patient sample P49S 2 days after electroporation using the program DS-138 showed a percentage of 71 successfully edited genome. Knockout was found in around 58 percent of the cells.

Ten days post-electroporation, the knockout score increased to 79 percent.

Figure 5 to 13. Sanger sequencing analysis of AML primary patient samples after electroporation.

Each sequencing result is illustrated in six graphs A-F: **Graph A:** Edited Sanger trace two days after electroporation, **Graph B.** Edited Sanger trace ten days after electroporation. **Graph C.** Control Sanger trace (wild type). The dotted line indicates the cut site. The horizontal black line indicates the sgRNA guide sequence, and the horizontal red line indicates the Protospacer Adjacent Motif (PAM) site. The PAM sequence is the sequence that is used for the Cas9 nuclease. A successfully edited gene region often shows several traces overlaying each other after the cut site. **Graph D.** Distribution of indel sizes in the edited population two days after electroporation. **Graph E.** Distribution of indel sizes in the entire edited population ten days after electroporation. The sequences are listed in order of percentage of genome edited by the same indel. The dotted line indicates the cut site. **Graph F.** Summary of gene editing efficiency showing percentage of indels and knockout score each for two and ten days after electroporation. The indel percentage is equivalent to the editing efficiency in a mixed population of cells and a general indication of how well a given sgRNA cuts under the present conditions. The knockout score considers the proportion of cells with either a frameshift or 21+ bp indel, which will most likely lead to a functional KO of the targeted gene (see chapter 2.6.11.).

The editing efficiencies of all cell lines investigated with every assessed electroporation program at both time points are summarized in the following figure:

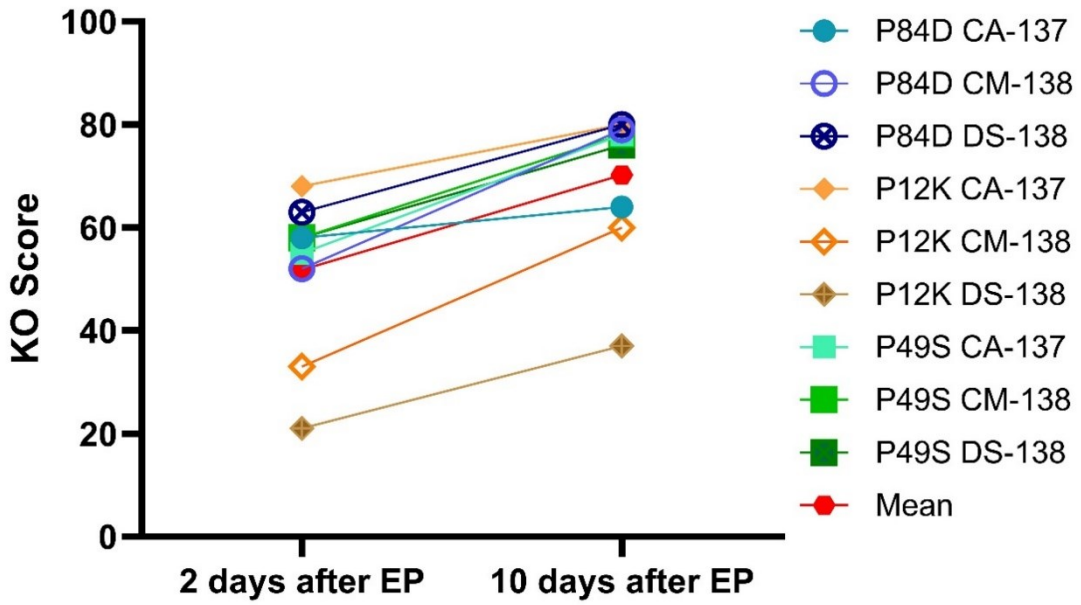

Figure 14. Summary of *BAALC* KO scores in AML primary patient samples 2 and 10 days after electroporation of three AML patient samples with each of three electroporation programs.

In summary, establishing a knockout of the *BAALC* gene in the AML primary patient cells P84D, P12K, and P49S through electroporation with three different nucleofection programs and chemically modified sgRNA was successful. Except for the patient sample P12K, which showed lower knockout rates with the programs CM-138 and DS-138, a knockout rate of over 50 percent was accomplished in all the patient samples after two days.

The knockout rate increased in each sample independent of the patient sample and electroporation program. The mean KO Score after 2 days was 51,7%, after 10 days it was 70,2%. Comparing theses scores, there was a significant increase (p= 0,017), suggesting that the knockout was stable and that the genome editing process after electroporation may not be completed after two days.

After successful establishment of BAALC KO in the de novo AML patients, we conducted the same protocol for the CN/AML patient sample. The gene editing efficiency was 47% (KO score 39%) (data not shown). Because of the low cell count, all cells were then used for the injection in NSG mice, so we could not conduct sequencing analysis on day 10.

We continued to measure the cell proliferation of AML primary cells with *BAALC* KO compared to their respective wild type cells.

3.3. *In vitro* proliferation analysis of *BAALC* knockout versus wild type cells

By manual cell count (see chapter 2.6.2.), we measured the proliferation of cells with *BAALC* knockout in comparison to wild type cells in the *BAALC*^{high} cell lines KG-1a (Fig.15) and Kasumi-1 (Fig.16) as well as in the AML primary patient samples P84D, P12K, and P84D over time (Fig.17).

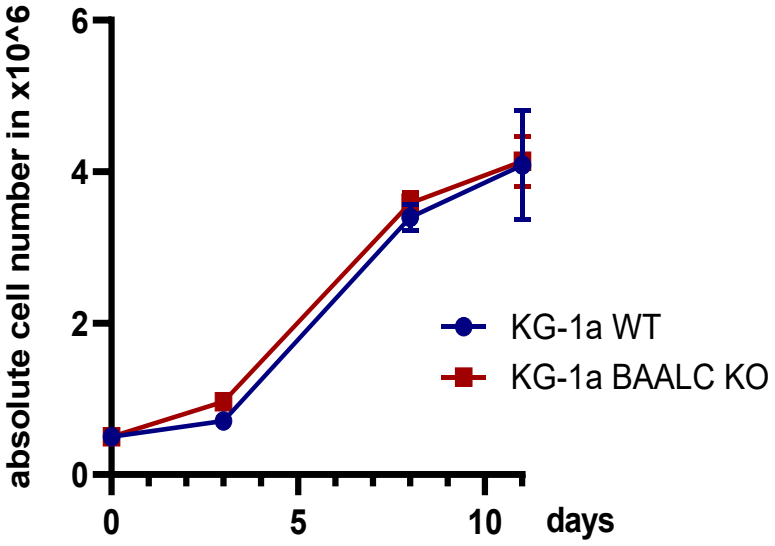

Figure 15. Proliferation assay of KG-1a WT vs *BAALC* KO.
KG-1a cells were electroporated with the program CA-137 with chemically modified sgRNA or no-template control and seeded in equal cell concentrations. After 3, 8 and 11 days the proliferation was measured via manual cell count. Confirmation of the knockout was done in advance with a stable knockout score between 87 and 89 percent. Data represent means ± SD from one experiment with triplicates.

After three days, KG-1a showed a tendency for a difference in proliferation between *BAALC* KO and WT cells (P= 0,00082) (see Fig.15). After eight and eleven days, there was no significant difference left between the proliferation of KO and WT cells.

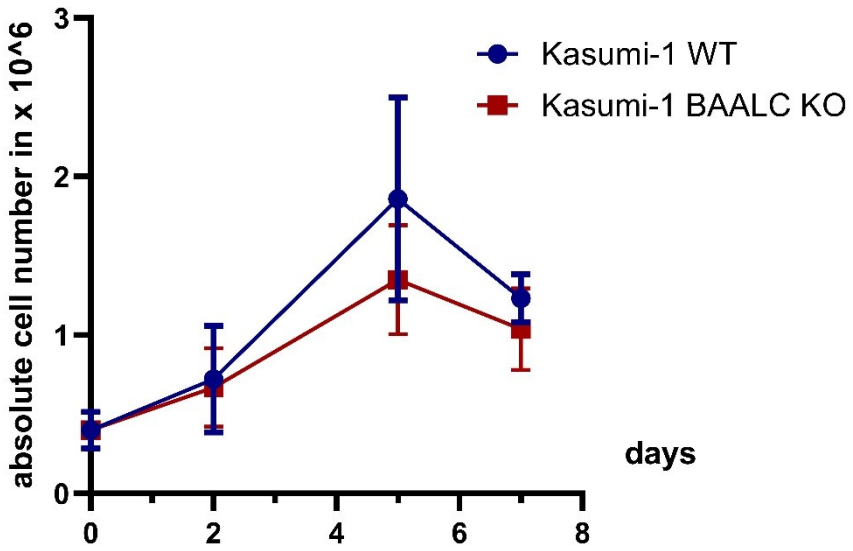

Figure 16. Proliferation assay of Kasumi-1 WT vs BAALC KO.
Kasumi-1 cells were electroporated with sgRNA. Single cell cloning was carried out by Masoud Nasri. The knockout was confirmed by sequencing analysis. Kasumi-1 WT and Kasumi-1 *BAALC* KO cells were seeded in equal cell concentrations. After 2, 5 and 7 days the proliferation was measured via manual cell count. Data represent means from two experiment with duplicates.

Kasumi-1 with *BAALC* KO also showed no significant difference in proliferation than Kasumi-1 WT for the observed time in culture (p>0,2) (see Fig.16).

A similar experiment was carried out with de novo AML primary patient samples. After three days, the proliferation was measured via manual cell count (see chapter 2.6.2.). Because of the limited resources of AML primary patient cells and the fact that we experienced the cells becoming adherent after around seven days in culture, the cell count could only be carried out till day three.

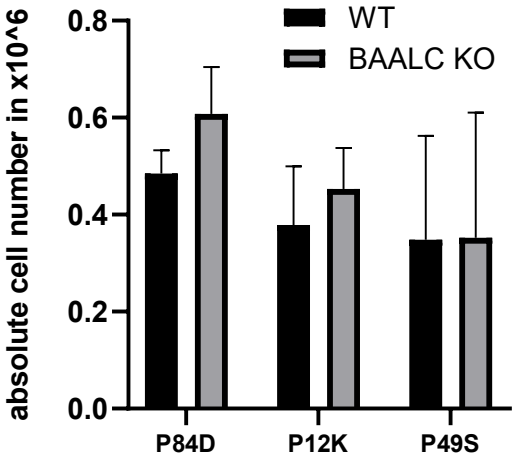

Figure 17. Proliferation assay of AML patient samples WT vs BAALC KO.
AML primary patient samples were electroporated with and without chemically modified sgRNA and seeded in equal cell concentration on feeder cells. After 3 days the proliferation was measured via manual cell count. 1x10^5 cells were removed for DNA isolation for confirmation of the knockout. Due to the small cell number the proliferation assay could not be continued after the removal of the cells. Data represent means ± SD from two experiments with duplicates.

The data indicates no difference in the proliferation of AML primary patient samples with *BAALC* KO vs. *BAALC* WT. (p>0,19) (see Fig.17).

In the *in vitro* experiments with the cell lines KG-1a and Kasumi-1 and the AML primary patient samples, there was no significant difference between *BAALC* KO cells and wild type cells.

Since leukemic cells often behave differently *in vitro* and *in vivo,* we aimed to analyze the proliferation of the *BAALC*^{high} cell line KG-1a, the cells of the three de novo primary AML patient cells, as well as the cells of a CN/AML-patient with each *BAALC* KO and WT in NSG mice.

3.4. *In vivo* proliferation analysis of *BAALC* KO cells in xenograft mice model

For the *in vivo* experiment, cells of the *BAALC*^{high} cell line KG-1a *BAALC* KO or WT were injected into the tail vein of NSG mice. After signs of leukemia, the mice were sacrificed, and the bone marrow was analyzed by FACS. The results are shown in the following graph:

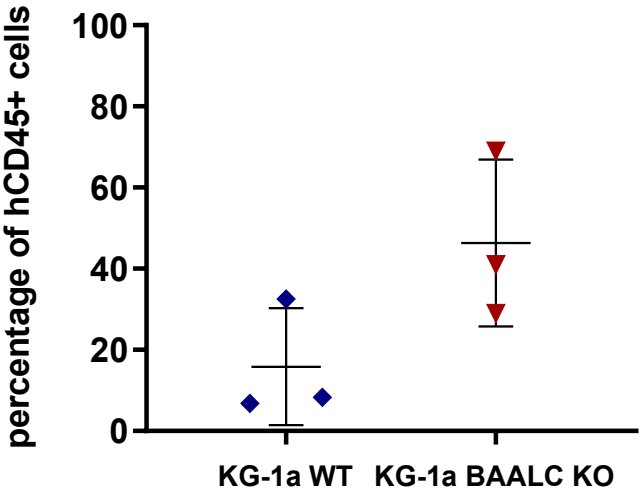

Figure 18. Engraftment of KG-1a WT vs. BAALC KO in NSG mice 7 weeks after injection. Injection of respectively 5 Mio cells of KG-1a WT or *BAALC* KO into the tail vein of NSG mice 4 hours after radiation with 225 Gray. After signs of leukemia, the mice were sacrificed. The bone marrow was strained into cell suspensions and stained with antibodies for FACS. The percentage of human CD45+ cells in each sample was analyzed by FACS. Data represent means ± SD from one experiment with three mice in each group.

The data indicates no significant difference between the engraftment of KG-1a wild type and the *BAALC* knockout cells in NSG mice (p=0,10) (see Fig. 18).

Similarly, the engraftment analysis was carried out with each de novo AML primary patient sample P84D, P12K, and P49S.

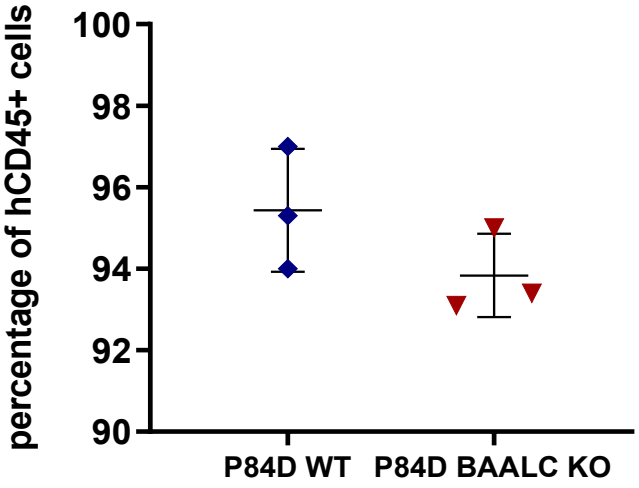

Figure 19. Engraftment of P84D WT vs. BAALC KO in NSG mice.
Injection of 1.2 Mio P84D cells of WT or *BAALC* KO each mouse into the tail vein of NSG mice. After signs of leukemia, which developed 4 weeks after injection, the mice were sacrificed. The bone marrow was strained into cell suspensions and stained with antibodies for FACS. The percentage of human CD45+ cells in each sample was analyzed by FACS. Data represent means ± SD from one experiment with three mice in each group.

There was no statistically significant difference between the engraftment of P84D *BAALC* KO vs. WT cells (p=0,20) (see Fig. 19).

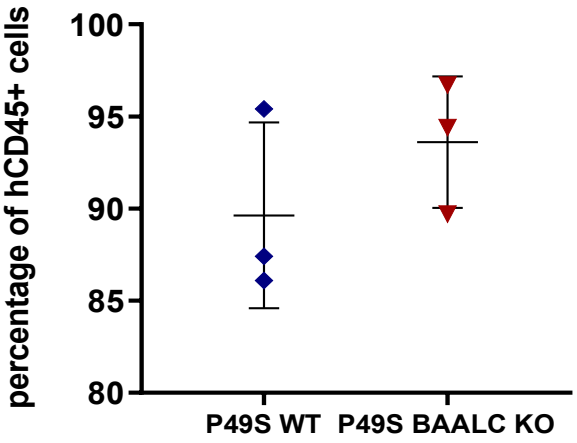

Figure 20. Engraftment of P49S WT vs. BAALC KO in NSG mice 5 weeks after injection. Injection of 0.5 Mio P49S cells of WT or *BAALC* KO each mouse into the tail vein of NSG mice. After signs of leukemia, which developed 5 weeks after injection, the mice were sacrificed. The bone marrow was strained into cell suspensions and stained with antibodies for FACS. The percentage of human CD45+ cells in each sample was analyzed by FACS. Data represent means ± SD from experiment with three mice in each group.

There was also no statistically significant difference between the engraftment of P49S *BAALC* KO vs. WT cells (p=0,32) (see Fig. 20).

The cells of the third de novo AML primary patient sample P12K were also injected into the tail vein of NSG mice. After eleven weeks, the mice did not develop any signs of leukemia and were sacrificed. After FACS analysis, we could confirm that neither the wild type nor the *BAALC* knockout cells did engraft in the mice.

In summary, the xenograft mice model injected with *BAALC* KO and WT de novo AML primary patient samples P84D and P49S showed no significant engraftment difference. The AML primary patient sample P12K, the CN/AML patient sample, and the Kasumi-1 cell line could not be evaluated since neither WT nor *BAALC* KO cells engrafted in these experiments.

3.5. Analysis of *in vivo* behavior of *BAALC* KO AML cells in zebrafish model

Other than NSG mice we used zebrafish embryos to investigate the behavior of BAALC KO and WT Kasumi-1 cell line *in vivo*. To enable tracking the *BAALC* KO and WT Kasumi-1 cells within the transparent zebrafish embryos, we labeled the cells with CFSE labeling dye. Subsequently, the labeled cells were injected into zebrafish embryos 24 hours post-fertilization (see Fig. 21).

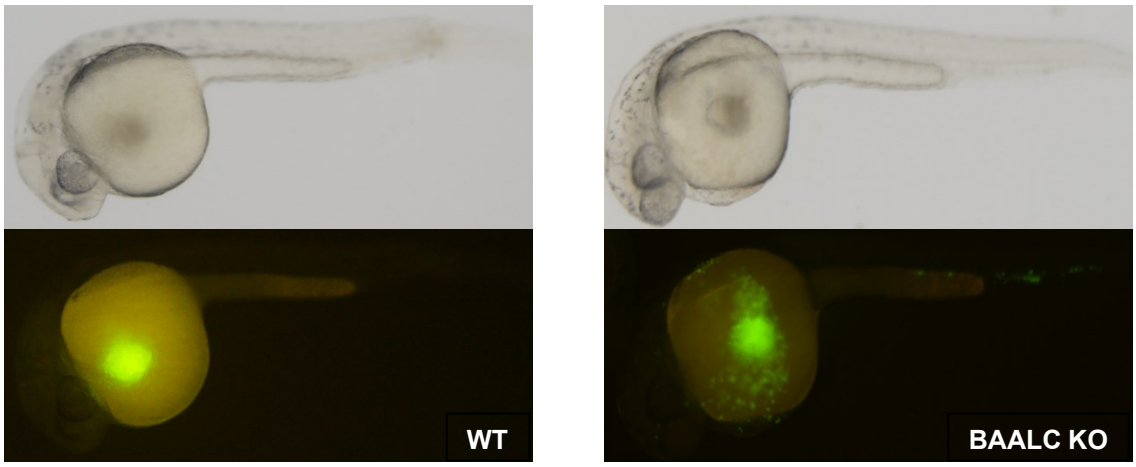

Figure 21. Two representative examples of thirty Zebrafish embryos 24h post fertilization after injection with CFSE-labeled cells of Kasumi-1 wild type (left) or Kasumi-1 BAALC KO (right).

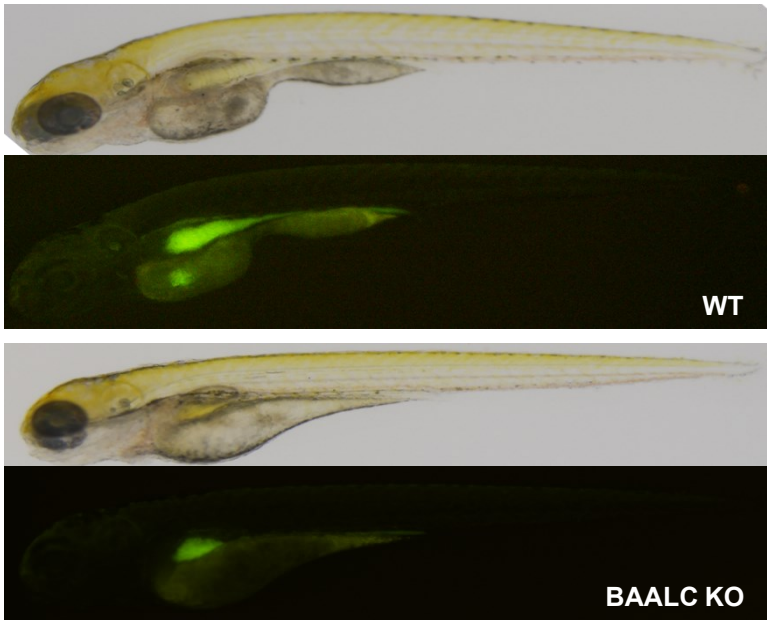

Figure 22. Two representative examples of Zebrafish embryos (n=30) 48h after injection with CFSE-labeled cells of Kasumi-1 wild type (top) or Kasumi-1 BAALC KO (bottom).

After 48h incubation (see Fig 22), the zebrafish embryos were strained through a cell strainer to create a cell suspension, which was then analyzed by FACS.

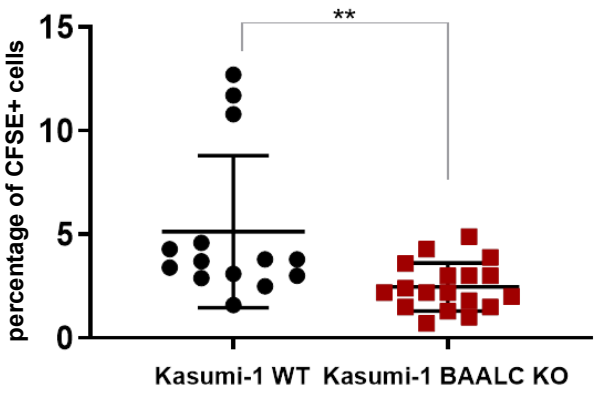

Figure 23. Engraftment of Kasumi-1 WT vs. BAALC KO in zebrafish embryos 48 hours after injection.

After 48h incubation the zebrafish embryos were strained through a cell strainer to create a cell suspension which was then analyzed regarding their percentage of CFSE-labeled cells by FACS. Data represent means ± SD from two independent experiments, each dot represents a pooled cell suspension of 5 embryos.

The data shows that zebrafish embryos injected with Kasumi-1 cells with *BAALC* KO had a significantly lower percentage of CFSE-positive cells than those injected with Kasumi-1 cells wild type (p=0,0068). This result indicates that the cells with *BAALC* KO had lower engraftment capacity in the zebrafish embryos than the WT cells.

3.6. Drug treatment with MEKK1 inhibitors

BAALC causes the induction of cell cycle progression through its interaction with the MEK-ERK signaling pathway. By binding MEKK1 it leads to a constant ERK activation [36] (see Chapter 1.3.3).

The following three drug candidates were selected by Benjamin Dannenmann to observe the effects of intervening in this signaling cascade.

As MEKK1 inhibitors, we used the MEK1 and MEK2-inhibitors U0126 and AZD6244. AZD6244, also known as Selumetinib, in certain concentrations is a specific MEK1-inhibitor with a lower IC50 than U0126. As a further option for a therapeutic approach for *BAALC*^{high} AML, we chose CMPD1, a non-ATP-competitive, selective inhibitor of the p38α-mediated M2Ka phosphorylation.

Benjamin Dannenmann has identified CMPD1 through a connectivity map analysis from RNA-sequencing data by comparing transcriptomes of CN/AML and CN/AML *BAALC* KO HSPCs. Drug candidates were assessed by introducing a gene expression profile similar to *BAALC* KO. “A selective inhibitor of p38a-mediated MK2a phosphorylation, CMPD1, was the first hit” [32]

We tested the effect of AZD6244, CMPD1, and U0126 each in three concentrations in comparison to DMSO control on cell viability of the *BAALC*^{high} AML cell line Kasumi-1, the three *BAALC*^{high} de novo AML patient samples as well as a healthy donor sample LPH27. The cell viability was measured after four days of treatment via CellTiter-Glo® Luminescent Cell Viability Assay (see Fig.24-29).

While the MEKK1 inhibitor U0126 did not show a significant effect on the *BAALC*^{high} Kasumi-1 cell line or the *BAALC*^{high} de novo AML patients in comparison to its effect on healthy donor LPH27 the MEKK1 inhibitor AZD6244 had a significant effect in the highest chosen concentration. The non-ATP-competitive, selective inhibitor of the p38α-mediated M2Ka phosphorylation CMPD1 achieved the highest drug effect. These results were partially published by Dannenmann et al. [32].

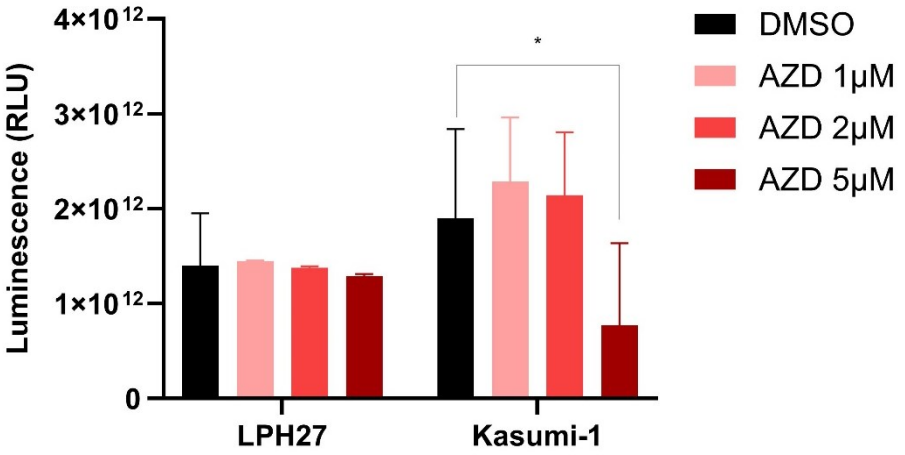

Figure 24. Cell viability of Kasumi-1 and healthy donor LPH27 upon treatment with AZD6244. The cell viability was measured after 4 days of treatment with AZD6244 in three concentrations (1µM, 2µM and 5µM) via CellTiter-Glo® Luminescent Cell Viability Assay. Each graph shows data that represent means ± SD from two independent experiments, each performed in triplicates.

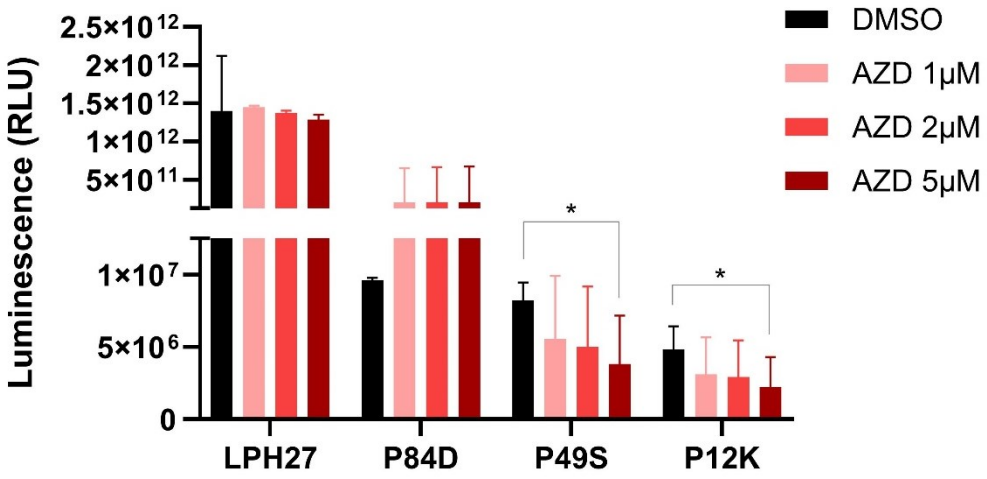

Figure 25. Cell viability of de novo AML patients P84D, P49S, P12K, and healthy donor LPH27 upon treatment with AZD6244.
The cell viability was measured after 4 days of treatment with AZD6244 in three concentrations (1µM, 2µM and 5µM) via CellTiter-Glo® Luminescent Cell Viability Assay. Each graph shows data that represent means ± SD from two independent experiments, each performed in triplicates.

AZD6244 showed a significant effect on the cell viability of the *BAALC*^{high} AML cell line Kasumi-1 (Fig.24) and two of the *BAALC*^{high} de novo AML patient samples (Fig.25). In contrast, the cells of the healthy donor were unaffected.
These results have been partially published by Dannenmann et al [32].

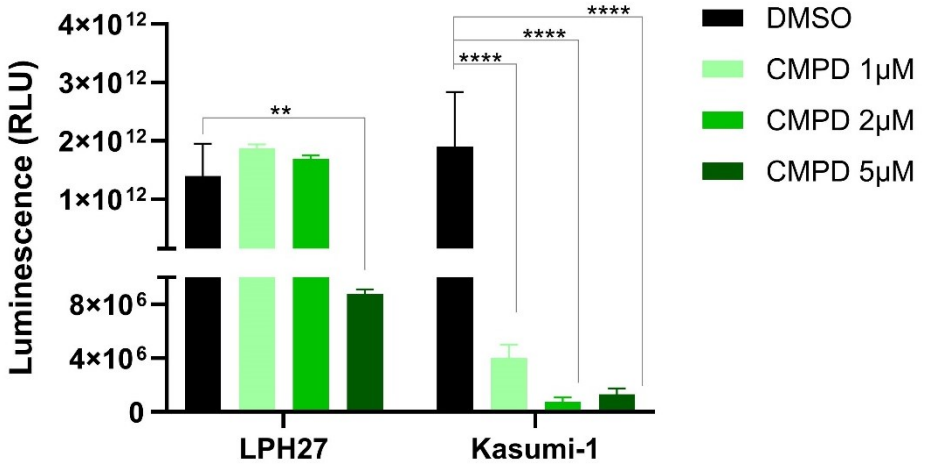

Figure 26. Cell viability of Kasumi-1 and healthy donor LPH27 upon treatment with CMPD1. The cell viability was measured after 4 days of treatment with CMPD1 in three concentrations (1µM, 2µM and 5µM) via CellTiter-Glo® Luminescent Cell Viability Assay. Each graph shows data that represent means ± SD from two independent experiments, each performed in triplicates.

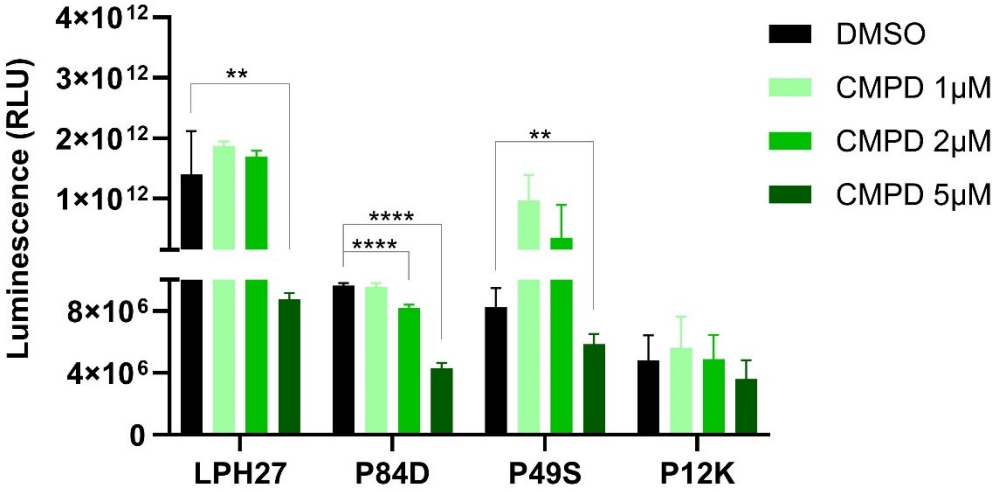

Figure 27. Cell viability of de novo AML patients P84D, P49S, P12K, and healthy donor LPH27 upon treatment with CMPD1.

The cell viability was measured after 4 days of treatment with CMPD1 in three concentrations (1µM, 2µM and 5µM) via CellTiter-Glo® Luminescent Cell Viability Assay. Each graph shows data that represent means ± SD from two independent experiments, each performed in triplicates.

CMPD1 showed a highly significant effect on the cell viability of the *BAALC*^{high} AML cell line Kasumi-1 (Fig.26) and one of the *BAALC*^{high} de novo AML patient samples (Fig.27) in the lower concentrations. In contrast, the cells of the healthy donor were only affected in the highest concentration.

These results have been partially published by Dannenmann et al [32].

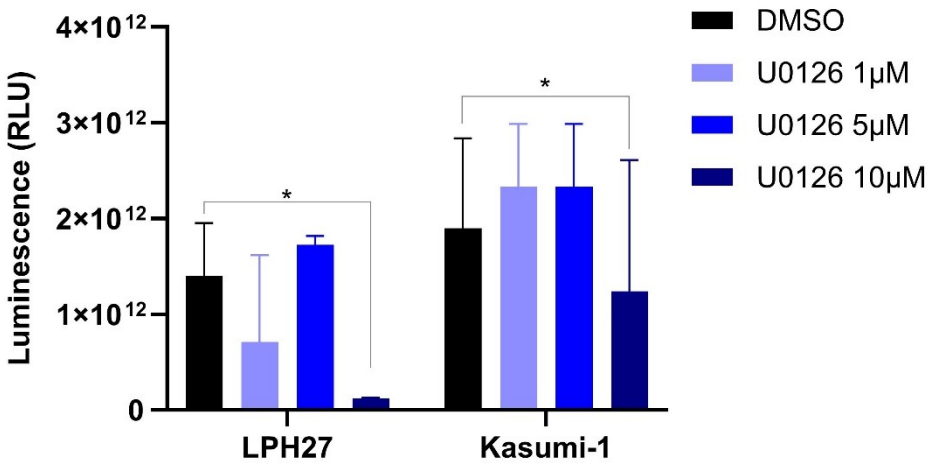

Figure 28. Cell viability of Kasumi-1 and healthy donor LPH27 upon treatment with U0126.
The cell viability was measured after 4 days of treatment with U0126 in three concentrations (1µM, 5µM and 10µM) via CellTiter-Glo® Luminescent Cell Viability Assay. Each graph shows data that represent means ± SD from two independent experiments, each performed in triplicates.

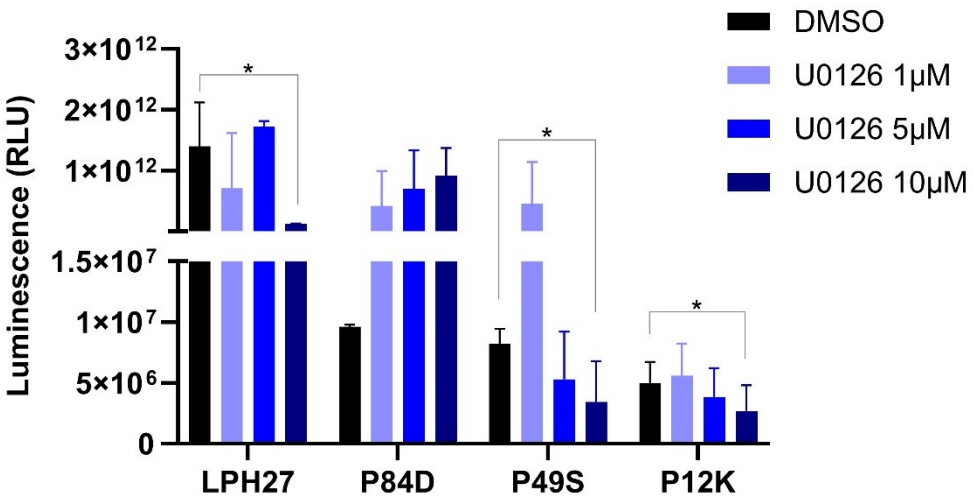

Figure 29. Cell viability of de novo AML patients P84D, P49S, P12K, and healthy donor LPH27 upon treatment with U0126.
The cell viability was measured after 4 days of treatment with U0126 in three concentrations (1µM, 5µM and 10µM) CellTiter-Glo® Luminescent Cell Viability Assay. Each graph shows data that represent means ± SD from two independent experiments, each performed in triplicates.

U0126 did not significantly affect the leukemic cells compared to the impact on the healthy donor cells (Fig.28 and Fig.29). These results have been partially published by Dannenmann et al [32].

4. Discussion

Acute myeloid leukemia (AML) is the subtype of leukemia with the highest mortality rate in adults. It has been vastly researched in the last decades, yet the mortality rate has only decreased slightly [1]. The more understanding has been reached about AML, the more genetic alterations have moved into focus [42]. These genetic alterations have been relevant not only for prognosis but also for models of leukemogenesis and treatment, especially of cytogenetically normal AML [8].

One of these genetic alterations that several research groups have studied is the high expression of the *brain and acute leukemia cytoplasmic (BAALC*) gene in AML blasts.

4.1. Role of *BAALC* in leukemogenesis

Although there has been a lot of research about *BAALC*, the role of *BAALC* in leukemogenesis is not yet disclosed. There are many implications of a significant role of *BAALC* in leukemogenesis: In AML patients, high *BAALC* expression correlates with the expression of other stem cell markers such as *CD34*, *CD133,* and *KIT,* suggesting *BAALC* to be associated with immature hematopoietic cells. [30]

Furthermore, high *BAALC*-expressing AML patients were more probable to carry well-known mutations, namely *FLT3-ITD, CEBPA,* and *MLL-PTD,* than low *BAALC*-expressing AML patients. [30]

Yet, there has been no proof that high *BAALC* expression increases the ability of self-renewal or proliferation in HSPC. Nevertheless, the consideration of *BAALC* promoting leukemogenesis remains, as there is evidence of *BAALC* impeding myeloid differentiation. [31]

The leukemic transformation of SCN has been investigated in the past [22, 32, 43, 44]. SCN is, in most cases, caused by mutations of the *ELANE* gene, which encodes for neutrophil elastase. Patients with SCN develop MDS or AML in 22% of all cases after 10 years. [19]

Mutations that are known to exacerbate malignant development in CN patients are *CSF3R* and *RUNX1* mutations.

RUNX1 encodes the transcription factor RUNX1, which plays an essential role in myeloid hematopoiesis. *CSF3R* encodes for the colony stimulating factor 3 receptor in granulocytes. Skokowa et al. found a high frequency of cooperativity of *CSF3R* and *RUNX1* mutations in many CN/AML patients, suggesting a pathway of leukemogenesis with “mutations in the hematopoietic cytokine receptor (G-CSFR) in combination with the second mutations in the downstream hematopoietic transcription factor (RUNX1)”[23].

Dannenmann et al. generated patient-specific induced pluripotent stem cells (iPSCs*)* to study stepwise leukemia development in congenital neutropenia in an *in vitro* model [32]. Multiple iPSC clones were created with different combinations of mutations (*ELANE, CSF3R, RUNX1*), and the proliferation and differentiation of these clones were analyzed [32].

BAALC expression was confirmed to be elevated in primary CN/AML blasts of five patients with *CSF3R* and *RUNX1* mutation in comparison to CD34+CD33+ BM cells of CN patients. This was also the case for the two generated CN/AML iPSC-derived HPSC lines. Dannenmann et al. registered a salient increase in *BAALC* expression when introducing *RUNX1* mutations into healthy donor CD34+ cells. [32]

Knockout of each of four genes (*BAALC, RUNX1, CD109, HPGDS*) in one CN/AML iPSC-derived HPSC line was used to investigate the genes that were linked to leukemic transformation. Of these four genes, only the knockout of BAALC resulted in an increase of differentiation and a decrease in proliferation in the CN/AML iPSC-derived HPSCs, while no such effect was observed in healthy donor iPSCs. [32]

The transcriptomes of both CN/AML iPSCs lines with *BAALC* WT and *BAALC* KO were compared. Dannenmann et al. found “a dramatic shift in gene expression signature” and that *BAALC* KO “partially restores CN phenotype irrespective of *RUNX1* mutation type” (missense or truncated) [32]. Also, cell cycle-regulating processes like oxidative phosphorylation and genes like protooncogene *MYC*, transforming growth factor β *TGF-ß*, cell cycle-regulating *E2F*, and *G2M* checkpoint-controlling pathways were discovered to be influenced by *BAALC* in CN/AML. [32]

In this study, we analyzed the role of *BAALC* overexpression on leukemogenesis and the behavior of leukemic blasts *in vitro* and *in vivo.*

We observed the effect of *BAALC* knockout on the proliferation rate of leukemic blasts *in vitro*. We expected blasts with *BAALC* knockout to have a lower proliferation rate than blasts with *BAALC* wild type. *In vivo,* we compared the engraftment capacity of AML cells with and without *BAALC* knockout in zebrafish embryos and NSG mice. The engraftment capacity of AML blasts is associated with the prognosis and, therefore, the aggressiveness of the AML [45]. We expected that *BAALC* KO would lead to less engraftment capacity.

In vivo, experiments with primary AML or primary CN/AML blasts are rare because of the restrictive resources of patient samples and methodological difficulties of cell cultivation and engraftment.

In our experiments, we used two AML cell lines, three primary de novo AML cells, and one CN/AML patient sample. The two AML cell lines we chose were Kasumi-1 and KG-1a. In the Kasumi-1 cell line, the fusion gene *RUNX1-RUNX1T* has been identified [46]. KG-1a has numerous mutations, e.g., *TP53,* but no mutation in the *RUNX1* gene [47, 48]. We also used samples of three pediatric patients with de novo AML P12K, P49S, and P84D independent of whether or not they carry a *RUNX1* mutation. The CN/AML patient sample carried an inherited *GPT1* mutation, a *RUNX1* missense mutation *(K83Q)*, and a *CSF3R* mutation *(Q720X).*

The establishment of a protocol for *BAALC* KO in primary AML samples was the first step in our experiments. After many attempts, a protocol was established with a stable knockout of *BAALC* in two AML cell lines and all three AML patient samples with no significant reduction of cell viability. We then proceeded to analyze the proliferation of KG-1a *BAALC* WT vs. *BAALC* KO and the three de novo AML patient samples with a *BAALC* WT vs. *BAALC* KO *in vitro*. We did not see a significant difference in proliferation between the two groups.

In vivo, we saw a significant difference between Kasumi-1 WT and *BAALC* KO in our zebrafish embryo experiment. In mice, however, neither the WT nor the *BAALC* KO Kasumi-1 cells did engraft. Two of three de novo AML patient

samples that did engraft in the mice showed no difference between *BAALC* WT and KO.

Our results did not support the hypothesis that *BAALC* KO would reduce proliferation in *BAALC*^{high} AML *in vitro* or *in vivo*. Our results suggest that *BAALC* overexpression may have less impact on the behavior of AML blasts than previous research suggested. Although considering the low number of patients and the limitations of this study, this conclusion could be disproportionate.

In this study, we only observed one factor of cell behavior, namely the proliferation of the blasts. Studying the differentiation status of the AML blasts could be an approach for further studies.

Considering the research of Dannenmann et al., the effect of high *BAALC* expression could also be dependent on *RUNX1* mutations. In our experiments, we had both samples with and without *RUNX1* mutations.

Kasumi-1 cell line and the CN/AML patient sample both had a *RUNX1* mutation. In the *in vivo* experiment with zebrafish embryos, Kasumi-1 with *BAALC* KO showed significantly less proliferation. Therefore, it could be assumed that *BAALC* KO reduced the ability to engraftment in the zebrafish embryos. Unfortunately, neither Kasumi-1 WT, Kasumi-1 *BAALC* KO, CN/AML *BAALC* WT nor CN/AML *BAALC* KO did engraft in mice.

The KG-1a cell line has no *RUNX1* mutation. For the primary AML patient samples, the *RUNX1* mutation status is unclear. These samples showed no difference between *BAALC* WT and *BAALC* KO in their engraftment capacity.

These results, combined with the results of Dannenmann et al., could indicate that the role of *BAALC* in leukemogenesis may depend on *RUNX1* mutation.

An approach to analyze the dependency of the role of *BAALC* in leukemogenesis from *RUNX1* could be comparing the effect of *BAALC* KO on AML cells with and without *RUNX1* mutation.

In this study, we also faced certain limitations, which are important to discuss when interpreting the results.

4.2. Methodological Difficulties

4.2.1. Cultivation of primary AML

In contrast to AML cell lines, primary AML and CN/AML samples are known to be difficult to cultivate in vitro [49]. The de novo primary AML patient samples in this study were grown in high cytokine media in a co-culture with stromal cells following a similar protocol as the protocol for “Generation, expansion, and drug treatment of hematopoietic progenitor cells derived from human iPSCs” later published by Dannenmann and Skokowa [50]. The high cytokine media contains the cytokines IL-6, SCF, TPO, FLT3L, and IL-3, and the stromal cells, also known as feeder cells, were modified to secret IL-3 and SCF at a constant rate.

Patient sample donations for research are rare, and these restricted resources allow only a certain number of cells to be used for the respective experiments. Numerous needs for sequencing of the cells shrank the number of cells even further. We could observe that the cells became more and more adherent to the stromal cells the longer they were in culture, often after three or four weeks, making correct manual cell count impossible.

There is yet no international standardized method for AML cultivation. Furthermore, there is the question of the influence of cultivation on the behavior of the cells.[49]

4.2.2. Selection of *BAALC*^{high} AML samples

While having no difficulty obtaining multiple AML cell lines, we could only access a limited number of primary AML samples from which to select BAALC^{high} AML samples. The *BAALC* mRNA expression of each cell line and AML primary sample was compared to the *BAALC* expression of CD34+ healthy donor cells.

Although there has been a lot of research about *BAALC* expression, there is no standard cut-off value to divide patient groups in low and high *BAALC* expression, making a comparison between the results of this study and other studies about *BAALC* less reliable.

4.2.3. Establishment of *BAALC* KO

To achieve a *BAALC* knockout in the AML cells, we tried several transfection methods, such as ribonucleoprotein electroporation with labeled tracerRNA with cell sorting and Lentivirus delivery of Cas9+sgRNA. In both cases, the method was unsuccessful because the knockout rate was low and the toxicity was high for the cells, resulting in large numbers of cell death (data not shown). Realizing the difficulties of transfection in primary AML cells, we established a protocol with selected less toxic electroporation programs and used a highly sensitive chemically modified sgRNA. The sgRNA (from Integrated DNA Technologies, USA) and the programs CA-137, CM-138, and DS-138 (of the Amaxa™ 4D-Nucleofector™ Protocol for unstimulated Human $CD34^+$ Cells with P3 Primary Cell 4D-Nucleofector® X Kit from Lonza, Switzerland) were found to be most tolerable for the primary AML cells. A knockout rate of over 50 percent was accomplished in all the patient samples after two days (except for one patient, P12K, which showed lower knockout rates with the programs CM-138 and DS-138). After ten days, the knockout rate increased in each sample independent of patient sample and electroporation program. After 48 days in culture, the electroporation program with the highest knockout rate for each patient sample was sent in for sequencing analysis, showing still stable knockout rates (data not shown). The process of gene editing using nucleofection with Cas9:sgRNA ribonucleoprotein is estimated to be almost completed after 3 days [51]. While achieving high and stable knockout rates in the primary AML cells, we still did not accomplish a hundred percent knockout rate, resulting in mixed cell populations of *BAALC* KO and *BAALC* WT. Other than the hypothesis of ongoing gene editing two days after nucleofection, the stable knockout rate could also be interpreted in the sense that *BAALC* WT did not have a proliferative advantage over *BAALC* KO. It could even be argued that in the mixed cell population, cells with *BAALC* KO seemed to have a proliferative advantage over *BAALC* WT due to the increasing knockout scores over time in these populations.

Moreover, we could not prove that the BAALC protein was no longer present in the cells. With a knockout stable for more than two days, the probability of eliminating the majority of the BAALC protein can be estimated to be high. To prove

the absence of BAALC protein, one could use western blot on the *BAALC* knock-out cells. At the time of our experiments (2019), there were no antibodies for western blot analysis.

4.2.4. Engraftment in NSG mice

For the *in vivo* experiments in NSG mice, we used the *BAALC*^{high} cell line Kasumi-1, KG-1a, three primary AML patient samples, and a CN/AML patient sample. 2-4 weeks after the injection, peripheral blood of the mice was analyzed by FACS to assess the leukemia engraftment. Depending on the leukemia engraftment in the peripheral blood samples and the clinical signs of leukemia in the mice, the mice were euthanized between 4 and 7 weeks after injection. The mice that did not show signs of engraftment were sacrificed around week 10 in our experiments. Of these six samples, only three engrafted successfully in the mice, creating a success rate of 50%.

Engraftment of leukemia in mice is known to be difficult. Generally, around 66% of injected NSG mice show AML engraft around 10–16 weeks post-transplantation [52].

Paczulla et al. studied the effect of prolonging the duration after transplantation on the percentage of successful engraftment. They found that extending the duration for up to 1 year allowed for engraftment of 95% of all AML. The group reported that “bone marrow biopsies taken at standardized time points failed to detect leukemic cells in 11/18 of cases that later showed robust engraftment”[53]. They concluded that leukemic blasts could persevere over months in an unobservable status without losing the potential to trigger the development of leukemia. [53]

The *BAALC*^{high} Kasumi-1 cell line, the primary AML patient P12K, and a CN/AML patient sample did not engraft in the mice in our experiments at week 10.

For the Kasumi-1 cell line, there are several recordings of successful engraftment in NSG mice by other research groups [54, 55].

Revising the transplantation protocol and a longer duration until analysis could have increased the chance of engraftment and would be advisable in future experiments.

4.3. *BAALC* downstream signaling pathway - Treatment of *BAALC*^{high} AML

In an attempt to reverse the effects of *BAALC* overexpression in leukemic blasts (e.g., induction of the cell cycle progression), Dannenmann et al. further investigated the signaling pathway downstream of *BAALC*.

Several transcription factors, for example, *RUNX1* and *SOX2*, as well MAPK14/p38α and CDK1/2 kinase pathways, were detected to be downstream of *BAALC* in two analyzed CN/AML patients. [32]

Verma et al. found a distinct link between *BAALC* expression in AML and *MYC* targets using GSEA[56]. *MYC* is a protooncogene and encodes for the transcription factor c-MYC, which is needed to balance the self-renewal and differentiation of hematopoietic stem cells. Overexpression of c-MYC has been found to lead to leukemia [57].

BAALC overexpression was also found to be associated with KRAS signaling pathway and inflammatory pathways like interferon-alpha and interferon-gamma pathways [56].

The improper activation of several oncogenic signaling cascades is a well-known part of AML pathogenesis. The Ras/Raf/mitogen-activated protein kinase (MEK)/extracellular signal-regulated kinase (ERK) pathway is activated in a significant amount of AML patients. [36]

Morita et al. found evidence that suggests *BAALC* acts as a scaffold-like molecule for the cytoplasmatic MEKK1, upstream ERK, and increases its kinase activity to phosphorylate ERK. They also found evidence that *BAALC* inhibits the reassociation of MKP3 and thereby sustains ERK activation (see Figure 1). [35, 36]

Constant ERK activation leads to proliferation and a block in differentiation. Inhibition of MEKK1 could, therefore, be an approach for the treatment of *BAALC*^{high} AML. [36]

Through Connectivity MAP analysis, Dannenmann et al. searched for drug candidates inducing a gene expression profile analogous to *BAALC* KO [32]. CMPD1, a selective inhibitor of p38α-mediated MK2a phosphorylation, was the most suitable candidate. Additionally, we used the MEK1 and MEK2-inhibitors U0126 and AZD6244.

The cell viability of *BAALC*^{high} leukemic blasts of three AML primary patients and the *BAALC*^{high} AML cell line Kasumi-1 was significantly reduced through treatment with CMPD1 compared to CD34+ healthy donor cells.
For AZD6244, we also registered a significant effect on the cell viability of two *BAALC*^{high} de novo AML patient samples and the *BAALC*^{high} AML cell line Kasumi-1. The results of the experiments regarding drug treatment with CMPD1 and AZD6244 have been partially published by Dannenmann et al. [32].
U0126 did not significantly affect the cell viability of the *BAALC*^{high} de novo AML patient samples and the BAALChigh AML cell line Kasumi-1 compared to CD34+ healthy donor cells.
The selective inhibitor of p38α-mediated MK2a phosphorylation CMPD1 and the MEK inhibitor AZD6244 may intervene in the ERK signaling pathway downstream of *BAALC* and could be further investigated as an approach for the treatment of *BAALC*-high AML patients.

4.4. High *BAALC* expression as a prognostic factor

Several studies have shown that patients with high *BAALC* expression are less likely to achieve complete remission, have shorter disease-free survival, and overall survival rates compared to patients with low *BAALC* expression. [30, 34]
Langer et al. found in 2008, in a multivariate study with 172 adult patients, that high *BAALC* expression predicted poor outcome independent from *FLT-3 ITD, NPM1, CEBPA* mutation status, and white blood cell count.[30]
Ewert et al. contradicted these findings with their study in 2014. The study included 339 patients and aimed to show whether or not the high *BAALC* expression had prognostic value if analyzed in combination with other well-established prognostic genetic markers in a multivariate analysis. [58]
Ewert et al. also found significantly lower overall survival and disease-free survival rates in the patient groups with high *BAALC* expression. However, in a multivariate analysis that included six variables, which were the combination of *FLT3* wild type and *NPM1*-Mutation, a *CEBPA* mutation, the availability of an HLA-identical bone marrow donor, the patient age, an *MLL-PTD* mutation, and the white blood cell count at the time of diagnosis high *BAALC* expression was not

found to be a significant prognostic factor for overall survival rates or disease-free survival rates in Ewert's multivariate analysis.[58]

FLT3-ITD and *NPM1* mutations are well-known and established prognostic factors whose use is recommended by the World Health Organization and the European Leukemia Net [8, 27]. Ewert found a significant association between high *BAALC* expression and *FLT3-ITD* mutation, a correlation between low *BAALC* expression and the prognostically favorable *NPM1* mutation, as well as a correlation between low *BAALC* expression and the prognostically favorable combination of *NPM1* mutation and *FLT3* wild type [58]. Ewert concludes that high *BAALC* expression has no new prognostic value compared to these well-known established prognostic markers and can be regarded as a surrogate marker [58].

In a meta-analysis of Xiao et al., 15 studies were analyzed to examine the reciprocity between *BAALC* gene expression and the prognosis of AML. Most of the analyzed studies also chose multivariate analysis to investigate the prognostic significance of the *BAALC* gene expression. [33]

In contrast to the findings of Ewert et al., the meta-analysis of Xiao et al. did not find a correlation between high *BAALC* expression and *FLT3-ITD* mutation. The correlation between low *BAALC* expression and *NPM1* mutation, which was stated by Ewert et al., was also found in the meta-analysis of Xiao et al. [33]

Furthermore, the meta-analysis found high *BAALC* gene expression could not be linked to white blood cell count or percentage of bone marrow blasts at the time of diagnosis or other clinical factors like gender or age. The pooled results confirmed that patients with high *BAALC* expression had lower overall survival, disease-free survival, and complete remission (after chemotherapy) rates. The meta-analysis of Xiao et al. concluded that high *BAALC gene* expression served as an independent poor prognostic indicator in adult patients with AML. [33]

Limitations of the meta-analysis of Xiao et al. were that from the retrieved 362 studies from the research literature, 347 of these studies were excluded because they did not meet the inclusion criteria. Also, the 15 included studies adopted different methods to detect *BAALC* gene expression. There was no standard cut-off value to divide patient groups in low and high *BAALC* expression. Most studies

used the median method according to the included patient cohort; therefore, the cut-off value differs from study to study. [33]

The studies of Langer et al. and Ewert et al. came to different conclusions, yet the fact that high *BAALC* expression is associated with poor prognosis is proved in both studies. The meta-analysis of Xiao et al. does confirm this. The value of high *BAALC* expression as an independent prognostic factor compared to the well-established prognostic factors *FLT3-ITD* and *NPM1* mutation is still doubtful. A new study with 111 patients in 2022 by Verma et al. also analyzed the correlation between BAALC and other genetic mutations. Like Xiao et al. they did not find a significant association between high *BAALC* expression and *FLT3-ITD* mutation and also found a correlation between low *BAALC* expression and *NPM1* mutation, as well as a correlation between low *BAALC* expression and the combination of *NPM1* mutation and *FLT3* wild type. Furthermore, Verma et al. found the highest *BAALC* expression in patients with *NPM1* wild type and *FLT3* wild type (*NPM1*-WT and *FLT3*-WT). In their multivariate study, they showed high *BAALC* expression to be the only variable (other variables: *CEBPA* mutation, age, gender, and the white blood cell count at the time of diagnosis) associated with low disease-free survival and overall survival rates in these (*NPM1*-WT and *FLT3*-WT) patients. Verma et al. suggest that *BAALC* gene expression could be used as a prognostic marker for outcome in patients with *NPM1* and *FLT* wild type. [56]

4.5. Conclusion and future projects

In this study, we aimed to investigate the role of *BAALC* overexpression on leukemogenesis and the behavior of leukemic blasts *in vitro* and *in vivo.*

We observed the effect of *BAALC* knockout on the proliferation rate of leukemic blasts *in vitro*. We expected blasts with *BAALC* knockout to have a lower proliferation rate than blasts with *BAALC* wild type. *In vivo,* we compared the engraftment capacity of AML cells with and without *BAALC* knockout in zebrafish embryos and NSG mice. We expected *the BAALC* knockout to lead to a lower engraftment capacity.

The results of our study could not support our hypothesis that *BAALC* KO would reduce proliferation in *BAALC*^{high} AML *in vitro* or engraftment capacity *in vivo* unconditionally. Considering the positive results regarding our experiments with Kasumi-1 and the relevant results achieved by Dannenmann et al. regarding *BAALC* KO in CN/AML in another group project under Professor Skokowa [32], we suspect that the role of *BAALC* overexpression in leukemogenesis and consequently cell behavior may depend on the cooperativity with *RUNX1* mutation.

Many researchers found evidence implying *BAALC* plays a key role in leukemogenesis. So far, this has only been verified by Dannenmann et al. for CN/AML with *RUNX1* mutation [32].

AML with *RUNX1* mutations shows distinct biology matching other high-risk AML. The Gene pattern of AML seems to be affected significantly by *RUNX1* mutations. *BAALC* overexpression is known to be associated with *RUNX1* mutations.[59]

Further experiments could analyze whether the effect of *BAALC* overexpression on AML is dependent on *RUNX1* mutation.

Genetic compensation could be another explanation for the lack of effect of *BAALC* KO in our experiments. Knockout of specific genes can lead to the upregulation of related genes as a direct consequence of the loss of protein function. Brolosy et al. state that knockouts did lead to a compensatory response in many cases, while knockdown of genes did less so.[60]

Following this theory, the knockdown of *BAALC* instead of knockout could be another approach for further experiments to prevent genetic compensation, which

could lead to not registering an effect of the downregulation of the gene expression.

There are many inconclusive studies regarding *BAALC* as a prognostic factor for AML. The proposition of Verma et al. to use *BAALC* gene expression as a predictive marker for outcome in patients with *NPM1* wild type and *FLT3* wild type seems like the most reasonable use of *BAALC* expression for the prognosis of AML at this time. [56]

Verma et al. also suggested that high *BAALC* expression in AML could partly be under epigenetic control. They concluded that *BAALC* overexpressing AML cases have distinct epigenetic alterations, which might be responsible for the poor prognosis in these patients.[56] The epigenetic control of *BAALC* could be an interesting field to study further.

The evidence of Morita et al. suggests that the *BAALC*-induced growth advantage of leukemic blasts they observed could rely on MEK-ERK signaling activity [35]. To intervene in this signaling pathway in *BAALC*^{high} AML, we tested the MEKK1 inhibitors AZD6244 and U0126 and CMPD1, a non-ATP-competitive, selective inhibitor of the p38α-mediated M2Ka phosphorylation.

CMPD1 and the dual MEK1 and 2 inhibitor AZD6244 significantly reduced the viability of *BAALC*^{high} AML cells in our study. These drugs could be further investigated as an approach for the treatment of *BAALC*^{high} AML patients.

5. Summary

Acute myeloid leukemia is a rare form of cancer with a high mortality rate that usually occurs in previously healthy patients. The emergence of the disease has been intensively studied. It is assumed that genetic alterations are the leading cause of leukemogenesis. These genetic alterations affect not only the clinical appearance of AML but also its prognosis and treatment.

The upregulation of *BAALC* gene expression is considered to be a significant negative prognostic factor in AML. Patients with *BAALC* overexpression are less likely to achieve complete remission and have shorter disease-free and overall survival rates. [30, 33, 34]

In this study, we aimed to analyze the role of *BAALC* overexpression on leukemogenesis and the behavior of leukemic blasts *in vitro* and *in vivo.*

Although scientific evidence suggests that *BAALC* impedes myeloid differentiation, there has been little to no proof of BAALC boosting self-renewal or proliferation in hematopoietic stem cells.[31, 32]

For our experiments, we used two *BAALC*^{high} AML cell lines, three *BAALC*^{high} AML primary patient samples, and one *BAALC*^{high} CN/AML patient sample. We established CRISPR/Cas9-mediated *BAALC* knockout in these cells and investigated the proliferation of the cells *in vitro*.

We could not find a significant difference in the proliferation rate between both groups.

In vivo, we compared the engraftment capacity of AML cells with and without *BAALC* knockout in zebrafish embryos and NSG mice.

Indeed, in the zebrafish xenotransplantation model, we observed a significant difference between *BAALC*-KO Kasumi-1 and the respective WT cells. The engraftment capacity of *BAALC*-KO cells was significantly reduced compared to *BAALC*-WT cells. In mice, however, *BAALC*-KO in KG-1a cells and two out of three AML patient samples showed no difference compared to their wild type counterparts. The Kasumi-1 cell line, one of the three AML patient samples, and the CN/AML patient sample did not engraft the mouse model.

Our results could not support the hypothesis that *BAALC* KO would reduce proliferation in *BAALC*^{high} AML in vitro or engraftment capacity in vivo

unconditionally. Considering the positive results regarding our experiments with Kasumi-1 (a *BAALC*^{high} AML cell line with *RUNX1* mutation) in zebrafish embryos and the relevant results achieved by Dannenmann et al. regarding *BAALC* KO in CN/AML (with *RUNX1* mutation) [32] we suspect that the role of *BAALC* overexpression in leukemogenesis and consequently cell behavior may depend on the cooperativity with *RUNX1* mutations.

In search of treatment options for patients with *BAALC*^{high} AML, we conducted experiments with three different drugs selected to intervene in the signal cascade downstream of *BAALC.* We treated the *BAALC*^{high} AML cells with CMPD1, an M2Ka inhibitor, and MEK1 and MEK2-inhibitors U0126 and AZD6244. We found that CMPD1 and AZD6244 reduced the cell viability of *BAALC*^{high} AML cells compared to healthy donor cells. The interference of drugs in the downstream pathway of *BAALC* could be an approach for further studies for the therapy of *BAALC*^{high} AML patients.

5.1. Zusammenfassung

Akute myeloische Leukämie ist eine seltene Krebserkrankung mit hoher Sterblichkeitsrate, die meist bei zuvor gesunden PatientInnen auftritt. Die Entstehung der Erkrankung wird und wurde intensiv erforscht. Es wird angenommen, dass Veränderungen des Genoms die Hauptursache der Leukämogenese sind. Diese Veränderungen beeinflussen nicht nur das klinische Erscheinungsbild der AML, sondern auch ihre Prognose und Therapie.

Die Überexpression des *BAALC* Gens gilt als markanter negativer Prognosefaktor für AML. Patienten mit *BAALC* Überexpression erreichen seltener eine komplette Remission und haben eine geringere krankheitsfreie und Gesamtüberlebensrate. [30, 33, 34]

Ziel dieser Forschungsarbeit war es die Rolle der *BAALC* Überexpression für die Leukämogenese und das Verhalten leukämischer Blasten *in vitro* und *in vivo* zu analysieren.

Obwohl es wissenschaftliche Belege gibt, die suggerieren, dass *BAALC* myeloische Differenzierung einschränkt, gibt es wenig Beweise, dass *BAALC* zur Selbsterneuerung oder Proliferation von hämatopoetischen Stammzellen führt [31, 32].

In unseren Experimenten verwendeten wir zwei AML-Zelllinien, drei primäre AML-Patientenproben und eine CN/AML-Patientenprobe. Alle verwendeten AML Blasten wiesen eine hohe *BAALC* Expression auf. Wir etablierten einen CRISPR/Cas9-vermittelten *BAALC* Knockout in diesen Zellen und untersuchten anschließend den Unterschied zwischen der Proliferationrate von *BAALC* Knockout versus Wildtyp *in vitro.*

Wir konnten hierbei keinen signifikanten Unterschied zwischen beiden Gruppen feststellen.

In vivo verglichen wir die Transplantationsfähigkeit von AML-Zellen mit und ohne *BAALC* KO in Zebrafisch Embryonen und NSG-Mäusen.

Tatsächlich zeigte das Zebrafisch-Xenotransplantationsmodell einen signifikanten Unterschied zwischen *BAALC* Knockout Kasumi-1 im Vergleich zu den jeweiligen Wildtyp-Zellen. Die Wachstumskapazität von *BAALC* Knockout Zellen im Vergleich zu *BAALC* Wildtyp Zellen war deutlich verringert. Bei Mäusen hingegen

zeigte *BAALC* Knockout in KG-1a-Zellen sowie in zwei von drei AML-Patientenproben keinen Unterschied im Vergleich zu ihren Wildtyp-Gegenstücken. Die Kasumi-1-Zelllinie, eine der drei AML-Patientenproben, und der CN/AML-Patient wuchsen im Mausmodell nicht an.

Unsere Ergebnisse konnten die Hypothese, dass BAALC Knockout die Proliferationsrate *in vitro* in AML mit hoher BAALC Expression verringern würde oder die Transplantationsfähigkeit *in vivo* herabsetzen würde, nicht uneingeschränkt bestätigen. Hinsichtlich der positiven Ergebnisse unserer Experimente mit der Kasumi-1 Zellinie (eine Zellinie die zusätzlich zu der erhöhten *BAALC* Expression eine *RUNX1* Mutation trägt) in Zebrafish Embyronen und der relevanten Ergebnisse die Dannenmann et al. bzgl. *BAALC* Knockout in CN/AML (mit *RUNX1* mutation) [32] erheben konnten, vermuten wir, dass die Rolle der *BAALC* Überexpression auf die Leukämogenese und das Zellverhalten von der Kooperation mit *RUNX1* Mutationen abhängig sein könnte.

Auf der Suche nach Behandlungsoptionen für Patienten mit BAALC Überexpression führten wir Versuche mit drei verschiedenen Wirkstoffen durch, die ausgewählt wurden, um in die Signalkaskade, die *BAALC* nachgeschaltet ist, einzugreifen. Wir behandelten AML Blasten mit hoher BAALC Expression mit CMPD1, einem M2Ka-Inhibitor, sowie den MEK1- und MEK2-Inhibitoren U0126 und AZD6244. Wir konnten feststellen, dass CMPD1 und AZD6244 die Zellviabilität von *BAALC*^{high} AML-Zellen im Vergleich zu gesunden Spenderzellen erniedrigten. Der Eingriff von Wirkstoffen in die Signalkaskade unterhalb von BAALC könnte weiter erforscht werden, um geeignete Therapien für Patienten mit *BAALC*^{high} AML zu finden.

6. References

1. Koch-Institut, R., *Krebs in Deutschland für 2019/2020.* 2023: p. 134-137.
2. Niemeyer, C., Eggert, A., *Pädiatrische Hämatologie und Onkologie*. 2018: Springer Verlag. 293-303.
3. Kean, L.S., R.J. Arceci, and W.G. Woods, *Acute Myeloid Leukemia*, in *Pediatric Hematology*, R.J. Arceci, I.M. Hann, and O.P. Smith, Editors. 2007. p. 360-383.
4. Bennett, J.M., et al., *Proposals for the classification of the acute leukaemias. French-American-British (FAB) co-operative group.* Br J Haematol, 1976. **33**(4): p. 451-8.
5. Amadori, S., et al., *Minimally differentiated acute myeloid leukemia (AML-M0): a distinct clinico-biologic entity with poor prognosis.* Ann Hematol, 1996. **72**(4): p. 208-15.
6. Bennett, J.M., et al., *Criteria for the diagnosis of acute leukemia of megakaryocyte lineage (M7). A report of the French-American-British Cooperative Group.* Ann Intern Med, 1985. **103**(3): p. 460-2.
7. Cree, I.A., *The WHO Classification of Haematolymphoid Tumours.* Leukemia, 2022. **36**(7): p. 1701-1702.
8. Khoury, J.D., et al., *The 5th edition of the World Health Organization Classification of Haematolymphoid Tumours: Myeloid and Histiocytic/Dendritic Neoplasms.* Leukemia, 2022. **36**(7): p. 1703-1719.
9. Loghavi, S., *SOHO State of the Art Updates and Next Questions—WHO Classification of Acute Myeloid Leukemia.* Clinical Lymphoma Myeloma and Leukemia, 2024. **24**(11): p. 752-758.
10. De Kouchkovsky, I. and M. Abdul-Hay, *'Acute myeloid leukemia: a comprehensive review and 2016 update'.* Blood Cancer J, 2016. **6**(7): p. e441.
11. Bonnet, D. and J.E. Dick, *Human acute myeloid leukemia is organized as a hierarchy that originates from a primitive hematopoietic cell.* Nature Medicine, 1997. **3**(7): p. 730-737.
12. Lane, S.W., D.T. Scadden, and D.G. Gilliland, *The leukemic stem cell niche: current concepts and therapeutic opportunities.* Blood, 2009. **114**(6): p. 1150-1157.
13. Long, N.A., et al., *Acute Myeloid Leukemia Stem Cells: Origin, Characteristics, and Clinical Implications.* Stem Cell Rev Rep, 2022. **18**(4): p. 1211-1226.
14. Reilly, J.T., *Pathogenesis of acute myeloid leukaemia and inv(16)(p13;q22): a paradigm for understanding leukaemogenesis?* Br J Haematol, 2005. **128**(1): p. 18-34.
15. Patel, J.P., et al., *Prognostic relevance of integrated genetic profiling in acute myeloid leukemia.* N Engl J Med, 2012. **366**(12): p. 1079-89.
16. Ley, T.J., et al., *Genomic and epigenomic landscapes of adult de novo acute myeloid leukemia.* N Engl J Med, 2013. **368**(22): p. 2059-74.
17. Hochman, M.J., et al., *Prognostic impact of secondary versus de novo ontogeny in acute myeloid leukemia is accounted for by the European LeukemiaNet 2022 risk classification.* Leukemia, 2023. **37**(9): p. 1915-1918.

18. Fioredda, F., et al., *The European Guidelines on Diagnosis and Management of Neutropenia in Adults and Children: A Consensus Between the European Hematology Association and the EuNet-INNOCHRON COST Action.* Hemasphere, 2023. **7**(4): p. e872.
19. Skokowa, J., et al., *Severe congenital neutropenias.* Nature Reviews Disease Primers, 2017. **3**(1): p. 17032.
20. Welte, K., C. Zeidler, and D.C. Dale, *Severe Congenital Neutropenia.* Seminars in Hematology, 2006. **43**(3): p. 189-195.
21. Rosenberg, P.S., et al., *Stable long-term risk of leukaemia in patients with severe congenital neutropenia maintained on G-CSF therapy.* Br J Haematol, 2010. **150**(2): p. 196-9.
22. Klimiankou, M., et al., *Role of CSF3R mutations in the pathomechanism of congenital neutropenia and secondary acute myeloid leukemia.* Ann N Y Acad Sci, 2016. **1370**(1): p. 119-25.
23. Skokowa, J., et al., *Cooperativity of RUNX1 and CSF3R mutations in severe congenital neutropenia: a unique pathway in myeloid leukemogenesis.* Blood, 2014. **123**(14): p. 2229-37.
24. Breems, D.A., et al., *Monosomal karyotype in acute myeloid leukemia: a better indicator of poor prognosis than a complex karyotype.* J Clin Oncol, 2008. **26**(29): p. 4791-7.
25. Estey, E.H., *Acute myeloid leukemia: 2019 update on risk-stratification and management.* Am J Hematol, 2018. **93**(10): p. 1267-1291.
26. Dohner, H., et al., *Diagnosis and management of AML in adults: 2017 ELN recommendations from an international expert panel.* Blood, 2017. **129**(4): p. 424-447.
27. Döhner, H., et al., *Diagnosis and management of AML in adults: 2022 recommendations from an international expert panel on behalf of the ELN.* Blood, 2022. **140**(12): p. 1345-1377.
28. Fenaux, P., et al., *Azacitidine prolongs overall survival compared with conventional care regimens in elderly patients with low bone marrow blast count acute myeloid leukemia.* J Clin Oncol, 2010. **28**(4): p. 562-9.
29. Tanner, S.M., et al., *BAALC, the human member of a novel mammalian neuroectoderm gene lineage, is implicated in hematopoiesis and acute leukemia.* Proc Natl Acad Sci U S A, 2001. **98**(24): p. 13901-6.
30. Langer, C., et al., *High BAALC expression associates with other molecular prognostic markers, poor outcome, and a distinct gene-expression signature in cytogenetically normal patients younger than 60 years with acute myeloid leukemia: a Cancer and Leukemia Group B (CALGB) st.* Blood, 2008. **111**(11): p. 5371-5379.
31. Heuser, M., et al., *Functional role of BAALC in leukemogenesis.* Leukemia, 2012. **26**(3): p. 532-536.
32. Dannenmann, B., et al., *iPSC modeling of stage-specific leukemogenesis reveals BAALC as a key oncogene in severe congenital neutropenia.* Cell Stem Cell, 2021. **28**(5): p. 906-922.e6.
33. Xiao, S.-J., et al., *Prognostic significance of the BAALC gene expression in adult patients with acute myeloid leukemia: A meta-analysis.* Molecular and Clinical Oncology, 2015. **3**(4): p. 880-888.

34. Weber, S., et al., *BAALC expression: a suitable marker for prognostic risk stratification and detection of residual disease in cytogenetically normal acute myeloid leukemia.* Blood Cancer Journal, 2014. **4**(1): p. e173-e173.
35. Morita, K., et al., *BAALC Acts As a Scaffold-Like Protein In The ERK Signaling Pathway and Promotes Leukemogenesis By Facilitating MEK–mediated ERK Activation.* Blood, 2013. **122**(21): p. 2509.
36. Morita, K., et al., *BAALC potentiates oncogenic ERK pathway through interactions with MEKK1 and KLF4.* Leukemia, 2015. **29**(11): p. 2248-56.
37. Gross, A.M., et al., *Selumetinib in Children with Inoperable Plexiform Neurofibromas.* N Engl J Med, 2020. **382**(15): p. 1430-1442.
38. Favata, M.F., et al., *Identification of a novel inhibitor of mitogen-activated protein kinase kinase.* J Biol Chem, 1998. **273**(29): p. 18623-32.
39. Knut and F. Alice Wallenberg. *The Human Protein Atlas*. www.proteinatlas.org 06.11.2024]; Available from: https://www.proteinatlas.org/ENSG00000164929-BAALC/cell+line#leukemia.
40. *Synthego | Full Stack Genome Engineering*. www.synthego.com 02.07.2024]; Available from: https://www.synthego.com/guide/how-to-use-crispr/ice-analysis-guide.
41. Livak, K.J. and T.D. Schmittgen, *Analysis of Relative Gene Expression Data Using Real-Time Quantitative PCR and the 2−ΔΔCT Method.* Methods, 2001. **25**(4): p. 402-408.
42. Mrózek, K., et al., *Clinical relevance of mutations and gene-expression changes in adult acute myeloid leukemia with normal cytogenetics: are we ready for a prognostically prioritized molecular classification?* Blood, 2007. **109**(2): p. 431-48.
43. Link, D.C., *Mechanisms of leukemic transformation in congenital neutropenia.* Curr Opin Hematol, 2019. **26**(1): p. 34-40.
44. Dannenmann, B., et al., *BAALC Is a Key Mediator of Leukemia Development in Congenital Neutropenia.* Blood, 2017. **130**(Supplement 1): p. 541-541.
45. Pearce, D.J., et al., *AML engraftment in the NOD/SCID assay reflects the outcome of AML: implications for our understanding of the heterogeneity of AML.* Blood, 2006. **107**(3): p. 1166-1173.
46. Kasai, F., et al., *Kasumi leukemia cell lines: characterization of tumor genomes with ethnic origin and scales of genomic alterations.* Hum Cell, 2020. **33**(3): p. 868-876.
47. *Cellosaurus cell line KG-1a (CVCL_1824).* Cellosaurus.org, 2015.
48. Pelliccia, F., V. Ubertini, and N. Bosco, *The importance of molecular cytogenetic analysis prior to using cell lines in research: The case of the KG-1a leukemia cell line.* Oncol Lett, 2012. **4**(2): p. 237-240.
49. Cucchi, D.G.J., Groen, R.W.J., Janssen, J.J.W.M., Cloos, J., *Ex vivo cultures and drug testing of primary acute myeloid leukemia samples: Current techniques and implications for experimental design and outcome.* ScienceDirect, 2020.
50. Dannenmann, B. and J. Skokowa, *Generation, expansion, and drug treatment of hematopoietic progenitor cells derived from human iPSCs.* STAR Protoc, 2022. **3**(2): p. 101400.

51. Hoellerbauer, P., et al., *A simple and highly efficient method for multi-allelic CRISPR-Cas9 editing in primary cell cultures.* Cancer Rep (Hoboken), 2020. **3**(5): p. e1269.
52. Sanchez, P.V., et al., *A robust xenotransplantation model for acute myeloid leukemia.* Leukemia, 2009. **23**(11): p. 2109-17.
53. Paczulla, A.M., et al., *Long-term observation reveals high-frequency engraftment of human acute myeloid leukemia in immunodeficient mice.* Haematologica, 2017. **102**(5): p. 854-864.
54. Huang, T., et al., *A murine model to evaluate immunotherapy effectiveness for human Fanconi anemia-mutated acute myeloid leukemia.* PLoS One, 2024. **19**(1): p. e0292375.
55. Chin, P.S. and C. Bonifer, *Modelling t(8;21) acute myeloid leukaemia - What have we learned?* MedComm (2020), 2020. **1**(3): p. 260-269.
56. Verma, D., et al., *BAALC gene expression tells a serious patient outcome tale in NPM1-wild type/FLT3-ITD negative cytogenetically normal-acute myeloid leukemia in adults.* Blood Cells Mol Dis, 2022. **95**: p. 102662.
57. Delgado, M.D. and J. León, *Myc roles in hematopoiesis and leukemia.* Genes Cancer, 2010. **1**(6): p. 605-16.
58. Ewert, J., *Die prognostische Bedeutung der BAALC-Genexpression bei der akuten myeloischen Leukämie des Erwachsenen*, in *Medizinische Fakultät*. 2014, Universität Ulm.
59. Gaidzik, V.I., et al., *RUNX1 Mutations in Acute Myeloid Leukemia: Results From a Comprehensive Genetic and Clinical Analysis From the AML Study Group.* Journal of Clinical Oncology, 2011. **29**(10): p. 1364-1372.
60. El-Brolosy, M.A. and D.Y.R. Stainier, *Genetic compensation: A phenomenon in search of mechanisms.* PLOS Genetics, 2017. **13**(7): p. e1006780.
61. *Mildred-Scheel-Doktoranden*. Krebshilfe.de 2024; Available from: https://www.krebshilfe.de/forschen/foerderung/foerderprogramme/nachwuchsfoerderung/mildred-scheel-doktoranden/.

7. Erklärung zum Eigenanteil der Dissertationsschrift

Diese Forschungsarbeit wurde in der Universitätsklinik Tübingen/Innere Medizin II unter der Betreuung von Prof. Dr. med., Julia Skokowa, PhD durchgeführt.

Die Konzeption der Studie erfolgte durch Professorin Julia Skokowa und Karl Welte in Zusammenarbeit mit den Betreuern dieser Forschungsarbeit Dr. Maksim Klimiankou, Dr. Ann-Christin Krahl, sowie Benjamin Dannenmann.

Sämtliche Versuche wurden nach Einarbeitung durch und mithilfe der Unterstützung von den Labormitgliedern von mir durchgeführt. Die Einarbeitung in die Forschung mit Zellkulturen und Mäusen erfolgte durch Dr. Ann-Christin Krahl. Die Auswahl, Observation und Präparation der Mäuse und die FACS Analyse der Zellen erfolgte in Zusammenarbeit mit Dr. Ann-Christin Krahl. Die genutzten Zebrafisch Embryonen wurden durch Narges Aghaallaei und Baubak Bajoghli bereitgestellt. Das Single Cell Cloning der Kasumi-1 Zellen erfolgte durch Masoud Nasri. Die Auswahl geeigneter Wirkstoffe für das Drug Treatment erfolgte durch Benjamin Dannenmann. Die statistische Auswertung erfolgte nach Anleitung durch Perihan Mir durch mich. Die Korrektur des Manuskripts erfolgte durch Dr. Maksim Klimiankou.

Ich versichere, das Manuskript selbständig verfasst zu haben und keine weiteren als die von mir angegebenen Quellen verwendet zu haben.

Stuttgart, den 20.02.2025

Jehan Mardan

8. Publication

Dannenmann B, Klimiankou M, Oswald B, Solovyeva A, Mardan J, Nasri M, Ritter M, Zahabi A, Arreba-Tutusaus P, Mir P, Stein F, Kandabarau S, Lachmann N, Moritz T, Morishima T, Konantz M, Lengerke C, Ripperger T, Steinemann D, Erlacher M, Niemeyer CM, Zeidler C, Welte K, Skokowa J. iPSC modeling of stage-specific leukemogenesis reveals BAALC as a key oncogene in severe congenital neutropenia. Cell Stem Cell. 2021 May 6;28(5):906-922.e6. doi: 10.1016/j.stem.2021.03.023. Epub 2021 Apr 23. Erratum in: Cell Stem Cell. 2023 Sep 7;30(9):1282. doi: 10.1016/j.stem.2023.07.015. PMID: 33894142.

II. Scholarship

This MD thesis was supported by the Mildred Scheel Doctoral Program of the German Cancer Aid. [61]

III. List of Figures

IV. List of Tables

V. Danksagung

Ich bedanke herzlich mich bei Professorin Julia Skokowa und Professor Karl Welte für das interessante Projekt, die aufmerksame Betreuung und die Möglichkeit in die Grundlagenforschung einzutauchen und so eine ungemeine Wertschätzung gegenüber Forschungsarbeit zu entwickeln. Ich bedanke mich darüber hinaus für die intensive Betreuung durch Maksim Klimiankou, welcher stets ein offenes Ohr für alle meine Fragen hatte, mir für meine Forschungsarbeit mit viel Geduld zur Seite stand und auch für die zeitaufwändige Korrektur dieser Schrift. Für die Teilhabe an seinem Forschungsthema und die Betreuung in Theorie und Praxis bedanke ich mich bei Benjamin Dannenmann. Ich bedanke mich auch bei meiner Betreuerin Ann-Christin Krahl, für die didaktisch tolle Einarbeitung in die Arbeit mit Zellen und Mäusen. Für die Einarbeitung in die Arbeit mit Zebrafisch Embryonen bedanke ich mich bei Narges Aghaallaei, Baubak Bajoghli und Larissa Doll. Ein Dank auch an alle technischen Assistenten, vor allem Regine Bernhard für die Einarbeitung in die Laborarbeit. Für die schöne Zusammenarbeit im Labor bedanke ich mich auch bei Masoud Nasri, Natalia Alejandra Borbarán Bravo, Malte Ritter, Betül Findik und Yun Xu. Ich bedanke mich bei der Deutschen Krebshilfe für die Aufnahme in das Mildred-Scheel-Doktorandenprogramm und der finanziellen Ermöglichung dieser Forschungsarbeit.

Ich danke meiner ehemaligen Mitbewohnerin Zeynep Mercan, für die schönen gemeinsamen Feierabende nach langen Tagen im Labor. Ich bedanke mich auch bei meiner Familie, insbesondere Sara Behr, Esma Mardan und Meriam Mardan für die mentale und physische Unterstützung zu allen Zeiten. Ich bedanke mich bei meinem Ehemann Muhammad Sahabi für die Geduld, als viele Wochenenden dem Schreiben zum Opfer fielen und die Motivation, die er mir schenkte.

Ein besonderer Dank geht an Perihan Mir, welche mir als Laborpartnerin nicht nur jede Frage beantwortete, die ich mich nicht traute, anderen zu stellen, sondern mir auch als große Schwester immer wieder aufbauend zur Seite stand, wenn mich mal der Mut verließ weiterzumachen.

Der größte Dank geht am meine Eltern Gülsan und Jamal Mardan. Die Liebe, die ich von euch spüren durfte, hat all dies erst ermöglicht. Danke für die vielen Opfer, die ihr in eurem Leben für meine Schwestern und mich gebracht habt.